

ANALYSIS OF NHEJ DNA REPAIR EFFICIENCY AND ACCURACY IN NEW
MUTANTS OF *SACCHAROMYCES CEREVISIAE*

by

Jennifer L. Lilley, B.S.

A thesis submitted to the Graduate Council of
Texas State University in partial fulfillment
of the requirements for the degree of
Master of Science
with a Major in Biochemistry
May 2015

Committee Members:

L. Kevin Lewis, Chair

Steve Whitten

Rachell Booth

COPYRIGHT

by

Jennifer L. Lilley

2015

FAIR USE AND AUTHOR'S PERMISSION STATEMENT

Fair Use

This work is protected by the Copyright Laws of the United States (Public Law 94-553, section 107). Consistent with fair use as defined in the Copyright Laws, brief quotations from this material are allowed with proper acknowledgment. Use of this material for financial gain without the author's express written permission is not allowed.

Duplication Permission

As the copyright holder of this work I, Jennifer L. Lilley, authorize duplication of this work, in whole or in part, for educational or scholarly purposes only.

ACKNOWLEDGEMENTS

I would like to first thank all who helped contribute to this project, specifically Janet Vela Ross, Sofia Warren, Whitney Wood, and Gilberto Guerrero. This project would not be complete without your assistance. To my committee members, Dr. Steve Whitten and Dr. Rachell Booth, for their advice and comments throughout this process. Also, to thank my parents Loretta Castro and James Lilley Jr. for their perpetual support and love. Thanks for cheering me on through this whole journey. I would like to thank Matthew DePugh for being my rock. You have bravely supported this endeavor and have been by my side the whole way through and I love you deeply for that. I especially would like to thank my research advisor, Dr. Kevin Lewis, for being my mentor. He taught me how to be a scientist and to shoot for the stars. You are a pivotal person in my life and I am profoundly grateful to have had the opportunity to work under such an intelligent person. Lastly, I would like to thank the entire Lewis lab from fall 2013-spring 2015. This has been one of the greatest experiences of my life. Though much work has been put into this thesis, the journey is the greatest reward I have. I love all of you and wish you the best in your life.

TABLE OF CONTENTS

	Page
ACKNOWLEDGEMENTS	iv
LIST OF TABLES	vi
LIST OF FIGURES	vii
CHAPTER	
I. INTRODUCTION	1
II. MATERIALS AND METHODS	12
III. RESULTS AND DISCUSSION	21
IV. SUMMARY AND CONCLUSIONS	56
REFERENCES	59

LIST OF TABLES

Table	Page
1. Oligonucleotides used for PCR reactions	20
2. DSB repair efficiencies determined using the new early stationary phase cell method	29
3. Established NHEJ mutant effects on DSB repair accuracy	30
4. Literature review of plasmid NHEJ efficiency	32
5. Summary of NHEJ mutant efficiency from past literature	33
6. DSB repair efficiencies of WT cells	34
7. Seventy-three new EcoRI-sensitive mutants identified by library screening	35
8. Results from first round of NHEJ efficiency testing for genes encoding proteins with nuclear functions	38
9. Results from first round of NHEJ efficiency testing for genes encoding proteins with non-nuclear or unknown functions	39
10. Mutant results of re-testing with reduction in DSB repair efficiency from first round of NHEJ testing	40
11. Results from first round of NHEJ accuracy testing for genes encoding proteins with nuclear functions	45
12. Results from first round of NHEJ efficiency testing for genes encoding proteins with non-nuclear or unknown functions	46
13. Mutants with reduced DSB repair accuracy from first round of NHEJ testing were tested a second time	47

LIST OF FIGURES

Figure	Page
1. EcoRI cleavage of DNA generated site-specific double-stranded breaks	3
2. Model of nonhomologous end-joining repair pathway in <i>Saccharomyces cerevisiae</i>	6
3. Simplified illustration of the homologous recombination pathway in <i>Saccharomyces cerevisiae</i>	8
4. <i>In vivo</i> expression of EcoRI from a plasmid using a <i>GAL1</i> promoter system	9
5. Genetic screening to identify DSB repair mutants	10
6. Improved protocol for transformation of stationary phase yeast cells with plasmid DNA	22
7. Plasmid DSB repair pathway	23
8. NHEJ DSB repair assay	24
9. Plasmid map of pRS315URA3	25
10. NHEJ DSB repair assay that permits quantitation of both the efficiency and accuracy of repair	27
11. Agarose gel electrophoresis of pRS315URA cut with Nco1	37
12. NHEJ efficiencies of mutants tested using opposite mating type strains	42
13. Agarose gel electrophoresis after PCR amplification of pFA6MX4 containing G418 ^r with 5' and 3' <i>ARP5</i> primers	49
14. Inactivation of a gene (<i>ARP5</i>) by insertion of an antibiotic resistant marker (<i>G418^r</i>)	50
15. Agarose gel electrophoresis of PCR fragments from G418 ^r chromosomal DNA	51
16. Dilution pronging assay to quantitate <i>mms22</i> -complex DNA repair mutants	53

17. Survival of library <i>mms22</i> , <i>rtt107</i> , <i>mms1</i> , and <i>rtt101</i> mutants after induction of EcoRI expression.....	54
18. Survival of library <i>mms22</i> , <i>rtt107</i> , <i>mms1</i> , and <i>rtt101</i> mutants on MMS and bleomycin	55

CHAPTER I

Introduction

Every life form contains deoxyribonucleic acid (DNA) coding sequences that encompass the blueprint for that organism. These sequences are polymers made up of monomer nucleotides. Each nucleotide is a deoxyribose sugar with a purine or pyrimidine base connected at the C1 position. Each nucleotide monomer is connected in a 5' to 3' direction by phosphodiester linkages in a sugar phosphate backbone, making DNA. The arrays of nucleic acids are paired with complementary strands arranged in the opposite direction with double helical secondary structure. The genetic information is quaternary in nature, only composed of four bases: guanine (G), cytosine (C), adenine (A), and thymine (T). G only pairs with C and A with T via hydrogen bonding, which is a strong enough intermolecular interaction to maintain structural integrity but is also weak enough to easily denature for replication and other cellular processes. Altogether, these polymers of DNA allow an organism to proliferate and withstand its internal and external environment. Thus, it is crucial for DNA sequences to be correct.

Genomic stability is continuously compromised by DNA damage caused by extra- and intracellular elements that manifest in several different ways. External assaults on DNA can be induced in the laboratory or experienced naturally. Radiation is a specific type of damage inducer that is a common laboratory method as well as an authentic damaging effect of sunlight through, specifically, ultraviolet (UV) light. In experimental

research, sparsely and densely ionizing radiation has also been shown to induce direct DNA damage through double-strand breaks (DSBs) and can be lethal to cells if DSB repair is inhibited (1,2). Ionizing radiation can attack the deoxyribose sugar, cleaving it from the polymer chain. Severed phosphodiester bonds carry an additional threat to cell survival because the overall DNA structure is destabilized, increasing the risk of mutation and cell death.

Other exogenous causes of DSBs are chemicals such as bleomycin, methyl methanesulfonate (MMS), and restriction endonucleases. Bleomycin is a member of a class of glycopeptide compounds found naturally in *Streptomyces verticillis* and is commonly used as an antitumor drug. Bleomycin causes DSBs by chelating metal ions, creating superoxides and radicals to attack the polymer (3). MMS is a DNA base methylating agent that primarily generates two products, 3meA and 7meG (4). Nuclease processing by base excision repair (BER) enzymes and pausing of DNA replication complexes, especially at 3meA sites, leads to single-strand breaks within each of the DNA strands.

Restriction endonucleases are enzymes commonly found in bacteria that cleave DNA strands at specific sites through catalytic hydrolysis of phosphodiester bonds within the DNA strands. EcoRI, specifically, is a bacterial restriction enzyme that recognizes a palindromic sequence that is 6 base-pairs (bp) in length. EcoRI-induced DSBs are beneficial in the investigation of cellular DSB repair efficiency because the breaks are controlled in quantity and quality. Breaks induced by restriction endonucleases may be blunt or have short (~1-5 nucleotides (nt)) overhangs. EcoRI generates DSBs that retain 4 nt 5' overhangs (Figure 1).

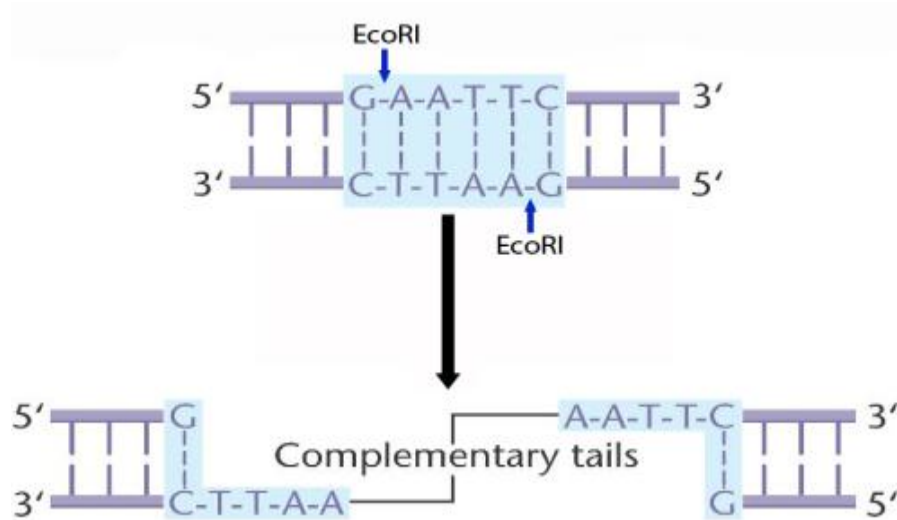


Figure 1. EcoRI cleavage of DNA generates site-specific double-stranded breaks.

In response to DSBs, eukaryotic cells have developed two major mechanisms for repair: homologous recombination and nonhomologous end-joining (5,6). Homologous recombination (HR) involves a strand invasion event where genetic information is physically swapped from one chromosome to another. Nonhomologous end-joining (NHEJ) is a simpler process whereby the broken strands are joined together, and, through the attachment of several binding factors to DNA, are ligated through the juxtaposition of the broken ends (7). Double-stranded DNA, once severed, typically has single strands extending out from the broken ends, which recruits NHEJ machinery to the DSB location (8). In *Saccharomyces cerevisiae* cells homologous recombination is the major DSB repair pathway and NHEJ is only dominant in G₁ phase, whereas in higher cells the reverse trend is expressed. NHEJ, though susceptible to errors, is a pathway utilized by G₁ cells in eukaryotes when there is no sister chromatid to act as template for homologous recombination.

Saccharomyces cerevisiae (budding yeast) is a unicellular eukaryotic organism with 16 chromosomes that has been a prominent model organism for genetic and molecular biology research for over 50 years. With its genome sequenced (9) and its ability to grow as either haploid or diploid cells, genetic investigation is cheaper and faster than with higher eukaryotes. In addition to high conservation of the sequences of genes and proteins used in basic cellular processes, *S. cerevisiae* cells have the capability of incorporating xenobiotic genes for *in vivo* analysis. This exploitation of the yeast cell provides a unicellular platform to investigate DNA repair mechanisms. Furthermore, rapid cell growth rates allow experiments to be performed quickly.

Several human disorders are associated with mutations in DSB repair genes. One important disease, severe combined immunodeficiency (SCID), is a genetic disorder characterized by low lymphocyte levels (lymphopenia) and growth defects. SCID is frequently caused by mutations in NHEJ repair genes. Therefore, investigations into yeast DSB repair complexes and mechanisms have solid effects that could have real clinical consequences in future research.

Figure 2 illustrates schematically the NHEJ protein-protein interactions mediating DNA DSB repair which is coordinated by the Ku, Mrx, and DNA ligase IV complexes. The model for *S. cerevisiae* NHEJ repair incorporates protein-protein interactions to process broken ends. Upon the emergence of a DSB, the Yku70/Yku80 complex is recruited. These Ku70 and Ku80 proteins bind nonspecifically to dsDNA ends, forming a ring-shaped heterodimer complex that encircles the ends of broken DNA, protecting them from nuclease degradation. The Mrx complex is then recruited by interactions between the Mre11/Rad50/Xrs2 proteins and the Ku proteins. Mrx tethers the broken ends to keep

them in proximity, recruiting the Dnl4 complex and ensuring that the Yku complex remains attached to the broken DNA ends. The Dnl4 complex consists of Dnl4, Lif1, and Nej1. The Dnl4 (DNA Ligase IV) protein contains the catalytic domain that ligates the broken DNA ends together. *In vivo* studies have illustrated the necessity of the correct alignment of these three major protein complexes for efficient NHEJ repair (10-12). Although these three components of NHEJ are needed to stage the repair event, genetic screening through mutation libraries have identified other proteins that can influence the efficiency of NHEJ repair (7,13).

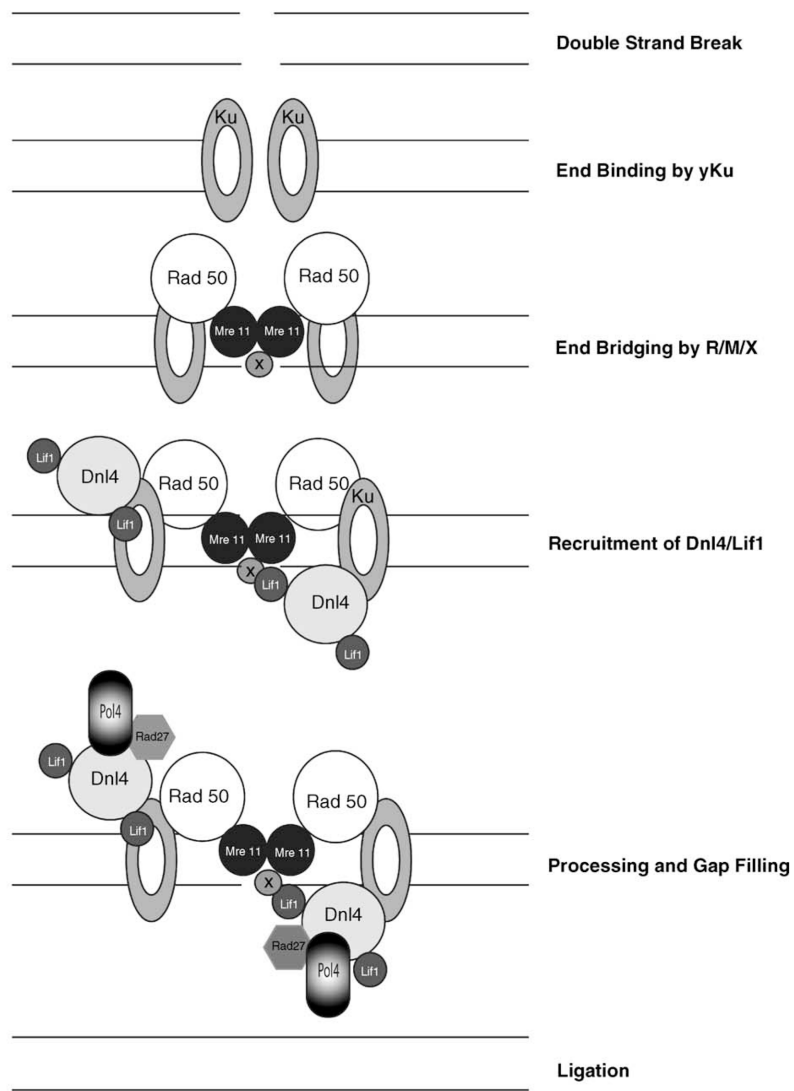


Figure 2. Model of nonhomologous end-joining repair pathway in *Saccharomyces cerevisiae* (14).

Unlike NHEJ, requiring only protein complexes, HR involves a homologous DNA molecule (usually a sister chromatid or a homologous chromosome) to provide a template for which duplication can materialize (Figure 3). Upon DSB formation, a resection event occurs at the 5' ends, creating long 3' single-stranded tails mediated by the Mrx complex and several other nuclease and helicase proteins (15). Single-stranded

DNA binding proteins bind to the DNA tails and recruit the binding of several other proteins. These proteins are part of the RAD52 group (Rad50, Rad51, Rad52, Rad54, Rad55, Rad57, Rad59, Mre11, Xrs2, Rdh54) that employ a homology search throughout the nucleus. A strand invasion into an unbroken DNA is then facilitated and exchange of genetic information is attained through formation and resolution of Holliday junctions (16).

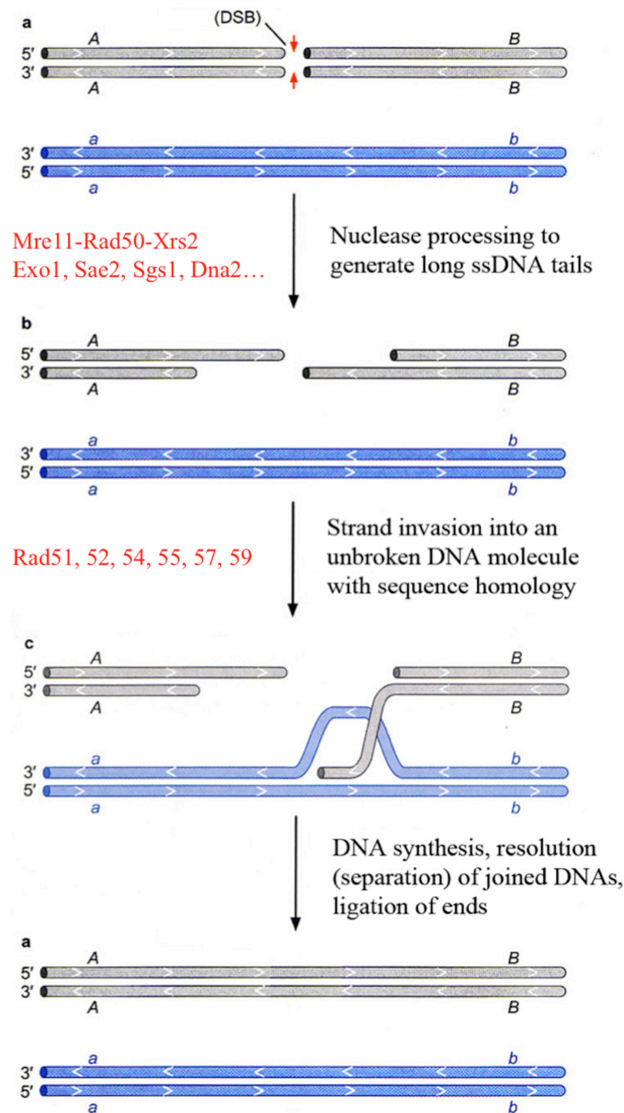


Figure 3. Simplified illustration of the homologous recombination pathway in *Saccharomyces cerevisiae*.

Previous screening of nearly 5,000 haploid yeast mutants, containing one non-essential gene deleted in each strain, revealed that 211 mutants were killed by exposure to low doses of gamma radiation (17, 18). The gamma sensitive mutants were later subjected to DSBs induced by *in vivo* expression of EcoRI endonuclease by the *GALI* promoter system in the Lewis lab (Figure 4) and the study found that 81 mutants were killed (13). Of the 81 mutants sensitive to EcoRI, eight of these mutants contained

inactivated genes that are already known to be involved in DSB repair pathways (Figure 5). These genes are part of the epistatic RAD52 group involved in HR DSB repair. Of the 73 “new” genes, several had already been linked to other cellular processes including transcriptional regulation, chromosome stability and segregation, DNA processing by nuclease enzymes, sister chromatid cohesion, and histone modification and remodeling (13).

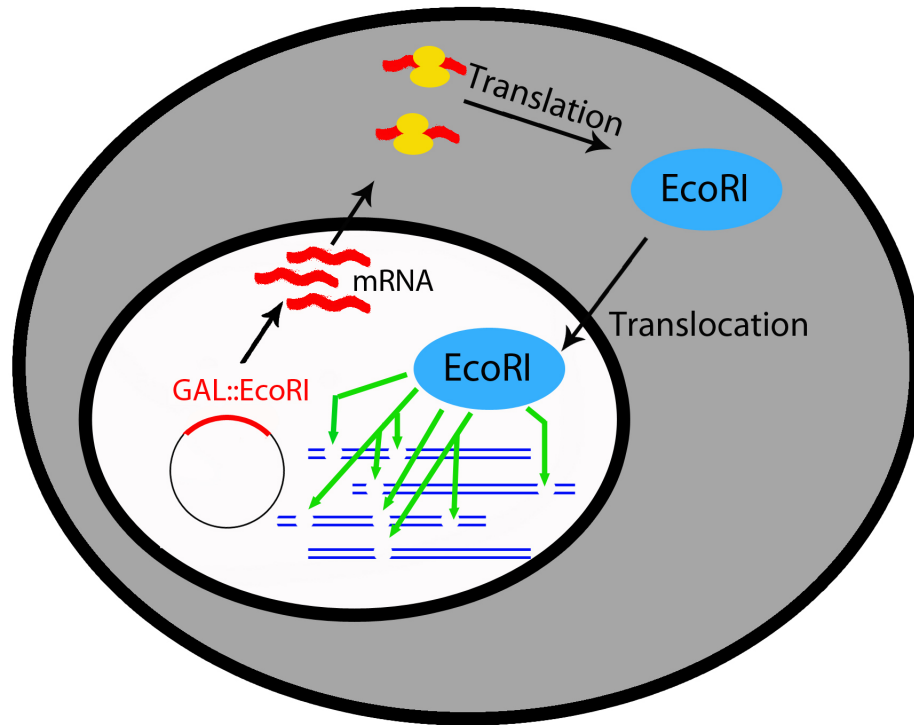


Figure 4. *In vivo* expression of EcoRI from a plasmid using a *GAL1* promoter system.

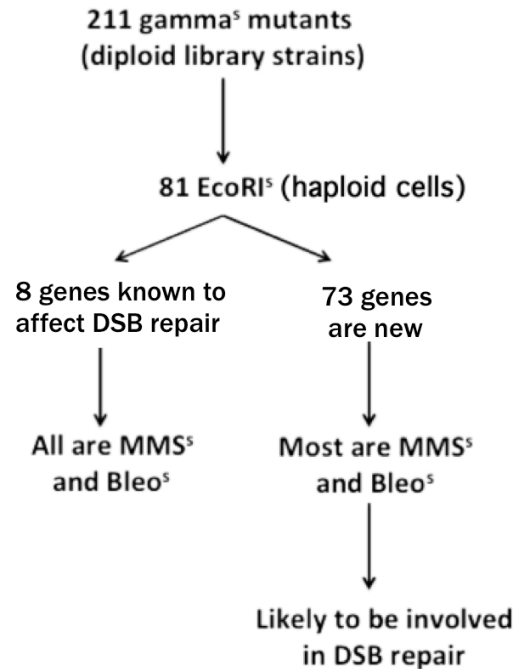


Figure 5. Genetic screening to identify DSB repair mutants.

The abilities of yeast mutants to perform DSB repair by NHEJ can be tested through a DSB repair assay using circular plasmid DNA (19). The assay involves lithium acetate-mediated rapid transformation of stationary phase yeast cells. Through the use of an improved yeast cell transformation protocol, NHEJ repair accuracy and efficiency can be better quantified through a larger range of fold-decrease or –increase (20). The lithium acetate-mediated assay historically requires dimethylsulfoxide (DMSO), polyethylene glycol (PEG), and lithium acetate (LiAc) to allow transformation of foreign plasmid DNA into stationary phase yeast cells. Improvements to this assay include the use of dithiothreitol (DTT) and incorporation of a rich broth recovery phase. DTT aids in disrupting disulfide bonds between cysteine residues on cell surface proteins. This allows for easier incorporation of plasmid DNA into the cell.

Plasmid assays have been used in past studies to identify yeast mutants that are defective in NHEJ repair. These investigations have revealed that *yku70*, *yku80*, *dnl4*, *lif1*, *nej1*, *rad50*, *mre11*, and *xrs2* strains typically exhibit reductions in repair relative to wildtype (WT) cells of about 10-20 fold (21-53). A few other mutants have been found to have modestly reduced NHEJ efficiency. These include cells lacking the *SIR* proteins Sir2, Sir3, and Sir4, which affect NHEJ indirectly by affecting expression of *NEJ1* (54).

mms22 is an EcoRI^S mutant that was identified in the Mckinney *et al.* study (13). The Mms22 protein is a subunit of the E3 ubiquitin ligase complex that has been linked to DNA replication and repair. Some proteins previously shown to physically interact with Mms22 are Mms1, Rtt101, and Rtt107 (55-57). Mms22 and Mms1 may influence DSB repair by replisome blocking (58), though their precise role is unclear. *mms22* mutants were found to be sensitive to EcoRI, MMS, bleomycin, and gamma radiation in the study by Mckinney *et al.* However, the sensitivities of strains with the other Mms22 complex subunit genes inactivated are unknown.

The goals of this project were to (a) perform a literature search of previously published assays that looked at any inactivated NHEJ repair genes, (b) modify an existing protocol for performing plasmid NHEJ assays in an attempt to improve it, (c) test the ability of 73 new mutants to repair DSBs by the NHEJ pathway, and (d) analyze DSB repair capabilities of a new mutant, *mms22*, that is known to be involved in polyubiquitination of proteins in the cell.

CHAPTER II

Materials and Methods

1. Materials

General Reagents

Omnipur (Darmstadt, Germany) supplied the agarose, EDTA, and bleomycin. Sonics-Vibra Cell (Newton, CT) provided the sonicator. Lithium acetate (LiAc), methylmethane sulfonate (MMS), dimethyl sulfoxide (DMSO), ampicillin, and RNase A were purchased from Sigma-Aldrich Chemical Co. (St. Louis, MO). The carrier DNA was a sonicated salmon sperm DNA (10 µg/ml) and was purchased from Stratagene (La Jolla, CA). Sodium dodecyl sulfate (SDS) and polyethylene glycol - 4000 (PEG) were purchased from Fluka Analytical (St. Louis, MO) and Tris was obtained from Shelton Scientific, Inc. (Peosta, IA). Ethidium bromide from IBI Scientific (Peosta, IA). The 2-Log DNA ladder (100 µg/µl) and NcoI were purchased from New England Biolabs (Ipswich, MA). Dithiothreitol (DTT) was purchased from Gold Biotechnology (St. Louis, MO). G418 sulfate (64.0 mg/mL) was obtained from Calbiochem (Darmstadt, Germany). NaOH was purchased from EM Science (Darmstadt, Germany). KOAC was obtained from Macron Chemicals (Phillipsburg, NJ).

Yeast strains and plasmids

Strains used for this project were haploid library derivatives of BY4742 (*MAT α ura3 Δ 0 leu2 Δ 0 his3 Δ 1 lyse2 Δ 0*) and BY4741 (*MAT α ura3 Δ 0 leu2 Δ 0 his3 Δ 1 met17 Δ 0*)

(59). All library yeast deletion strains were obtained from Open Biosystems (Huntsville, AL). Plasmids used in the NHEJ repair assays were pRS313 (*CEN/ARS HIS3*) and pRS315URA3 (*CEN/ARS LEU2 URA3*). Other plasmids used in this study include pGALEcoRI (YCpGAL::Rib) (*CEN/ARS URA3 GALIp::EcoRI*), pRS316 (*CEN/ARS URA3*) and pFA6MX4 (60-62).

Yeast Growth Media

Yeast cells cultivated for non-selective growth were harvested from YPDA plates (1% w/v bacto yeast extract, 2% w/v bacto peptone (or 2% w/v soy peptone), 2% w/v glucose, 2% w/v bacto agar, and 0.001% adenine). Overnight cultures were grown in YPDA broth that was prepared like YPDA plates but without agar. For sensitivity experiments, cells were grown on plates containing 1 mM MMS or 2 mM MMS from an 11.2 M stock solution. YPDA + bleomycin plates were also created for sensitivity assays using a stock solution of 0.5 mg/mL. Bleomycin plates were either 2 µg/mL or 4 µg/mL. Cells grown for plasmid selection were grown on synthetic media plates (0.17% w/v yeast nitrogen base without amino acids, 2% w/v glucose, 2% w/v bacto agar, and all essential amino acids minus those needed for selection). Synthetic glucose, raffinose, and galactose plates contained 2.2% w/v agar, leucine, adenine, histidine, lysine, uracil, and tryptophan. Unless noted otherwise, all sugars were 2%. For selection, various plates did not contain uracil, leucine, or histidine. *E. coli* cells were grown on LB with ampicillin plates using 1% w/v bacto tryptone, 0.5% w/v yeast extract, 0.5% w/v NaCl, 1.5% w/v agar, and 100 µg/mL ampicillin.

II. Methods

Gel electrophoresis

Gel electrophoresis was performed using 0.7-0.9% w/v agarose gels with 1X TAE (40 mM Tris base, 20 mM acetic acid, 1 mM EDTA) running buffer at ~140 V. The rig model was Life Technologies Horizon 11-14. Gels were stained with 0.5 µg/mL ethidium bromide (EtBr) for 15 minutes and photographed using an Alpha Innotech Red gel documentation system from ProteinSimple (San Jose, CA).

Early stationary phase yeast cell transformations

Transformation of plasmid DNA was performed with early stationary phase cells using a modification of the rapid lithium acetate/DMSO method introduced by Soni *et al.* (20, 63). Additional modifications were implemented to increase the transformants/µg DNA to ensure adequate colony number from poorly transforming mutant strains.

The Tripp *et al.* protocol used here was performed as follows:

1. Centrifuge overnight cultures grown in YPDA broth for 16,100 x g for 30 s.
Typically, 1.0 to 1.5 mL is used per assay tube.
2. Resuspend the pellet in 500 µL of 0.1 M DTT and incubate at 42° C for 20 min.
3. Sediment cells for 20 s and resuspend pellet with ~505 µL of PEG/LiAc solution containing plasmid and carrier DNA.

Per assay, add 400 µL 50% PEG + 50 µL 1 M LiAc + 10 µL 50 mM EDTA + 5 µL 1 M Tris (pH 7.5) + ~35 µL deionized water + 5 µL mg/mL boiled sonicated carrier DNA + 1-10 µL of plasmid DNA. Each master mix includes enough volume for one extra assay.

4. Add 56 μL DMSO and vortex to mix.
5. Incubate at 30° C, shaking, for 15 min.
6. Heat shock at 42° C for 15 min.
7. Centrifuge cells at 10,000 x g (usually ~8 s) and remove supernatant. (If cells are spun over 10,000 x g resuspension takes more time.)
8. Remove supernatant and wash pellet with 200 μL of deionized water.

(OPTIONAL: Resuspend cells in 500 μL YPDA and incubate, shaking, at 30° C for 30 min to help cells recover from the chemical incursion. After YPDA growout, sediment cells at 16,100 x g for 20 s and remove supernatant.)
9. Resuspend cells in 200-1000 μL deionized water, depending on the strain. Spread 5-100 μL onto selective plates, depending on the strain. To ensure adequate spreading, spot 50 μL of deionized water onto plates receiving 50 μL or less of cells prior to pipetting cells onto the plate.
10. Incubate plates at 30° C for ~3 days or at RT for 4-5 days.

Plasmid DNA midiprep by rapid alkaline lysis

Plasmid DNA was harvested from overnight cultures *E. coli* grown in LB + Amp broth shaking at 37° C. Cells were sedimented at ~5,000 x g for 5 min at 5° C. The bacterial cell pellet was resuspended with ice-cold TE (10 mM Tris, pH 8.0 + 1 mM EDTA), pH 8.0, and a solution of 0.2 N NaOH + 1% SDS was added, followed by incubation on ice for 2-3 min. Three molar KOAc was then added to the homogenous cell mixture and cells were incubated on ice for 3-5 min. Cells were then centrifuged at 18,000 x g for 10 min and the resulting supernatant was transferred to a new tube and mixed with 1 volume of propanol. The mixture was mixed and centrifuged at 18,000 x g

at 15° C for 5 min. The resulting pellet was washed with 70% ethanol for 3 min and dried for up to 60 min. The dried pellet was resuspended in 1.2 mL TE with 5 µL of 1 mg/mL RNase A. The solution was incubated at 37° C for 10-20 min and then stored at -20° C.

Plasmid DNA digestion

pRS315URA3 was digested with restriction endonuclease NcoI (10,000 U/mL) to induce a DSB in the *URA3* gene. Typical reactions involved 50 µL of plasmid DNA, 264 µL deionized water, 80 µL 5x potassium glutamate buffer (KGB), and 6 µL NcoI (10,000 U/mL) incubated at 37° C for up to 5 h. The digested plasmid was ethanol precipitated by adding 1/20th volume of 3 M NaOAc and 2.5 volumes of 100% cold ethanol to the DNA sample and incubating at -20° C for \geq 10 min. The DNA was centrifuged at 21,000 x g for 10 minutes, washed with 50 µL of cold 70% ethanol and re-spun for 3 min. After removing the supernatant the DNA pellet was dried in a Thermo Scientific Savant DNA120 Speedvac Concentrator for 10 min. The dry DNA pellet was stored in 50 µL TE + 100 µL deionized water. Plasmid DNA concentration was measured using a Life Technologies Qubit 2.0 Fluorometer according to the manufacturer's instructions. Before precipitation of the entire reaction, a fraction of the reaction was analyzed by 0.7% agarose gel electrophoresis to confirm proper digestion.

Chromosomal DNA purification

Yeast chromosomal DNA was extracted by using a SDS/EDTA/Tris (SET) protocol. Three milliliters of overnight cultures were centrifuged for 10 s at 16,000 x g and the supernatant was removed. The pellet were resuspended in 6% SET solution containing 6% SDS, 10 mM EDTA, and 30 mM Tris, and deionized water. The cell solution was incubated at 65°C for 15 min then transferred to ice where it was mixed with

150 μ L 3 M KOAc. The solution was centrifuged for 10 min at 21,000 x g and the supernatant was transferred to a new 1.5 mL tube. Five hundred microliters of isopropanol was added and vortexed with the solution. Cells were precipitated by centrifugation for two minutes and the supernatant was removed. Cells were 70% ethanol washed, dried, and resuspended in 50 μ L TE. One microliter of RNase A was added to cells at 37° C for 10 min to digest any remaining RNA molecules.

Survival Dilution Assay

Stock solutions of cells were prepared for each strain in 300 μ L deionized water. A 1/50 dilution was then prepared and sonicated at an amplitude of 2-3 for 8 s using a Vibra Cell Sonicator (model no. VCX130) from Sonics and Materials (Newtown, CT). Microscopic analysis was performed using a United Scope model M837T phase contrast microscope (Hopewull Junction, NY) to quantify the amount of cells in the 1/50 dilution sample. Cells were counted using a Bright-Line Hemocytometer from Hausser Scientific (Horsham, PA). Cells were counted in the upper-left, center, and lower-right 4x4 squares in a grid. Cells counts were averaged and calculated using the formula below:

$$\text{average cell count} \times 25 \times 50 \times 10^4 = \text{total cells/mL.}$$

The resulting value is the number of cells/mL in the original 300 μ L stock solution. A total of 2×10^7 cells in 220 μ L deionized water was serially diluted 1:5 fold in a 96-well plate and pronged onto plate media.

Nonhomologous end-joining efficiency

Seventy-three EcoR1^S mutants (13) were transformed with NcoI-cut pRS315URA3 (200 ng per transformation) using the high efficiency protocol of Tripp *et al.* (20). An uncut plasmid, pRS313 (~50 ng per transformation), was simultaneously

transformed into cells to act as a control for the transformation event. Each strain was tested in 3-4 separate assay tubes and each experiment was internally controlled with WT, BY4742 (*MAT α*) or BY4741 (*MATa*), and *dnl4* cells as positive and negative controls, respectively. All BY4742/BY4741 strains and their derivatives are *ura3 Δ 3 leu2 Δ 0 his3 Δ 0* and became His⁺ upon uptake of the pRS313 plasmid, Leu⁺ upon uptake and repair of the NcoI-cut pRS315URA3, and Leu⁺ Ura⁺ upon accurate repair of NcoI-cut pRS315URA3. Transformants were selected for repair efficiency on glucose minus leucine (Glu-Leu) and glucose minus histidine (Glu-His) plates. Colonies were counted from each plate. Colonies on Glu-Leu plates represented cells that repaired NcoI-cut pRS315URA3 and colonies on Glu-His plates represented cells that were transformed with the pRS313 plasmid.

Nonhomologous end-joining accuracy

NHEJ mutants were tested for accuracy of DSB repair by harvesting colonies from Glu-Leu plates used to select for repair of NcoI-cut pRS315URA3 transformation efficiency assays. Colonies were patched onto glucose minus leucine (Glu-Leu) and glucose minus uracil (Glu-Ura) plates to select for Ura⁺ cells. Only cells that accurately repaired the NcoI cut DSB exhibited a Ura⁺ phenotype and were, thus, qualitatively differentiated by patching onto Glu-Leu and Glu-Ura plates.

pGALEcoRI induction

Survival dilution studies using as described above was implemented to determine sensitivity to *in vitro* GAL induction of EcoRI expression. The plates used included 2% w/v raffinose minus uracil (Raff-Ura), 1% w/v raffinose and 2% w/v galactose minus uracil (1% Raff + Gal-Ura), 0.1% w/v raffinose and 2% w/v galactose

minus uracil (0.1% Raff + Gal-Ura), and 2% w/v galactose minus uracil (Gal-Ura) plates. Plates were dried for 30 minutes and incubated at 30° C for 2-3 days.

MMS and bleomycin survival studies

MMS and bleomycin sensitivity was tested in *mms22*, *mms1*, *rtt101*, and *rtt107* mutants using the survival dilution assay protocol. Mutant strains were pronged onto YPDA plates as control and YPDA + 1 M MMS, YPDA + 2 M MMS, YPDA + 2 µg/mL bleomycin, and YPDA + 4 µg/mL bleomycin plates. BY4742 and *rad50* cells were used as positive and negative controls, respectively.

Targeted gene disruption

Gene disruption of *ARP5* in BY4742 cells was initiated by PCR-amplification of the pFA6MX4 plasmid containing G418^r. PCR reactions were 50 µL total and contained 3 µL pFA6MX4 plasmid, 26 µL deionized water, 1 µM of each primer (Table 1) (Life Technologies), 0.25 mM dNTP's, 1X ThermoPol reaction buffer, 0.9 µL Taq DNA Polymerase (5,000 U/mL) (New England Biolabs Inc). The thermal cycler was a Bio-Rad T100 model and conditions were set at 94° C for 2 min for initial denaturation followed by 32 repeated cycles of 94° C for 30 s, 52° C for 40 s, and 72° C for 1.5 min. A final extension at 72° C for 7 min terminated the reaction. PCR products were analyzed by gel electrophoresis on a 0.9% w/v agarose gel. PCR products were ethanol precipitated by combining 4.5 µL 3 M NaOAc and 250 µL 100% cold ethanol, vortexed, and centrifuged at 21,000 x g for 10 min. Supernatant was removed and the resulting pellet was rinsed with 500 µL 70% cold ethanol and centrifuged for 2 min. The supernatant was removed and the pellet dried in the speedvac for 10 min. The dried pellet was resuspended in deionized water.

Plasmid DNA was then transformed into WT cells using the early stationary phase yeast cell transformation protocol described above. Cells were resuspended in 300 μ L deionized water and 150 μ L was spread onto YPDA plates. Cells were grown for 1-2 days at 30° C or until a “lawn” of cells were seen. Selection for G418^r was initiated by replica plating onto YPDA + G418 plates and, after incubating at 30° C for 2-3 days, colonies were streak purified and harvested for overnight cultures. Cells were used for chromosomal DNA purification as described above. Chromosomal DNA was subjected to PCR a second time using test primers and visualized on a 0.9% w/v agarose gel to test whether G418^r was incorporated into the *Arp5* region of yeast chromosomal DNA. Oligonucleotides used in this study are described in Table 1.

Table 1. Oligonucleotides used for PCR reactions

Primer	Sequence
gARP5a	CTGAAGAAATATTGGACTACACTTTTCATCATTGTTGGGAGTGGTACC AGATAACGGAATGTGACTGTCGCCCGTACATT
gARP5b	GTACCGGTAGGAAGGATTCCAGTGAATTCCTTCACAATACGTTCTT TCAATCCTGGACAAGTTCTTGAAAACAAGAATC
5-ARP5	TTCGAAGGACTCTGAACATAAGACGTATA
3-ARP5	AAGGCGTTTCAGTTTGCTGTCTCCTTAG

Primers used for amplification of G418^r begin with the letter g; primers used to confirm proper insertion of the gene into a chromosome begin with 5 or 3.

CHAPTER III

Results and Discussion

Past work in this lab identified 73 genes required for efficient repair of EcoRI-induced DSBs in yeast cells. Inactivation of many of these genes also caused cells to be sensitive to the chemicals bleomycin and MMS. The precise roles of most of these genes in DSB repair by NHEJ or HR is unknown. The goal of this project was to determine whether the 73 EcoRI^S mutants played a role in nonhomologous end-joining (NHEJ) DSB repair. To determine this, we used a plasmid repair assay that involves recirculation of cut plasmids that are transformed into early stationary phase yeast cells. Our lab has recently improved DNA transformation efficiencies of early stationary phase yeast cell cultures through the incorporation of DTT into a standard LiAc/PEG/DMSO mediated protocol (20). DTT reduces disulfide bridges formed between cysteine residues, disrupting cell surface proteins. This allows for greater incorporation of plasmid DNA into the cell.

With our improved transformation protocol, efficiencies of plasmid DNA transformations in WT cells were around 100,000-500,000 transformants/ μ g DNA. Previous investigations into transformation improvement in early stationary phase yeast cells (overnight cultures) only yielded 5,000-50,000 transformants/ μ g DNA (20, 63, 64). Adding incubatory periods with DTT and post-chemical treatment recovery in rich YPDA broth was found to produce a significant increase in transformation efficiency

(20). Figure 6 is a schematic that illustrates the steps in our improved transformation of early stationary phase yeast cells.

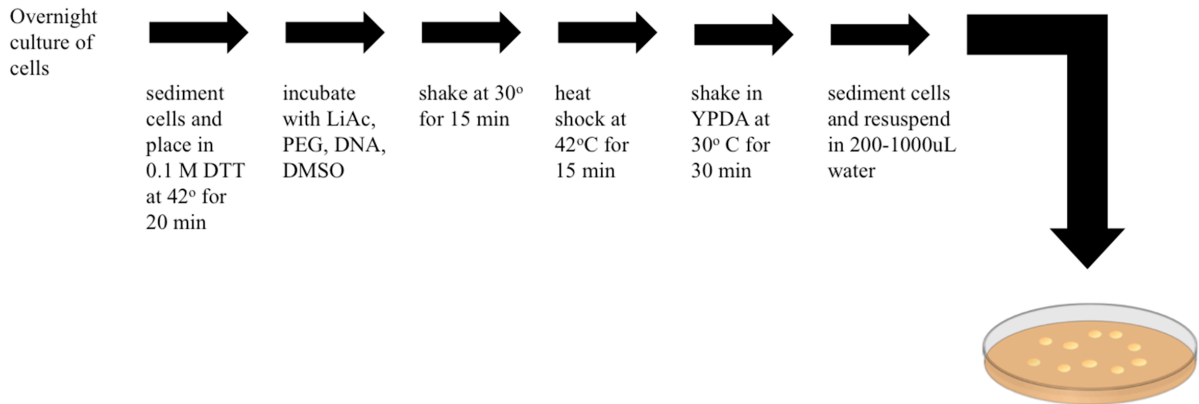


Figure 6. Improved protocol for transformation of stationary phase yeast cells with plasmid DNA. Rapid transformation protocol modified from (20, 63).

Novel additions and adjustments to the LiAc/PEG/DMSO transformation protocol require specific steps in order to achieve maximum efficiency. Overnight cultures of cells in rich (YPDA) broth ensure that *S. cerevisiae* cells will be in early stationary phase. Cells in a post-diauxic (early stationary) phase exist in roughly 50% G₁ phase and tend to be less efficiently transformed than log phase cells (65, 66). Thus, it is important to maximize the amount of DNA that enters the cell. Incubation with DTT at 42° C enhances entry into the cell after sedimentation. A heat shock at 42° C helps destabilize cell membranes and allows the cells to reprogram gene expression and synthesize proteins that aid in cell wall restructuring (67, 68).

A plasmid containing a single DSB can in theory be repaired (recircularized) by either of the two major DSB repair pathways, NHEJ or HR, after it is transformed into yeast cells (Figure 7). However, it is possible to specifically test the ability of cells to

repair a plasmid DSB by the NHEJ pathway. This was done by creating a restriction endonuclease-induced DSB in a plasmid such that there was no DNA sequence homology within several hundred bp on either side of the DSB. This type of assay is depicted in Figure 8.

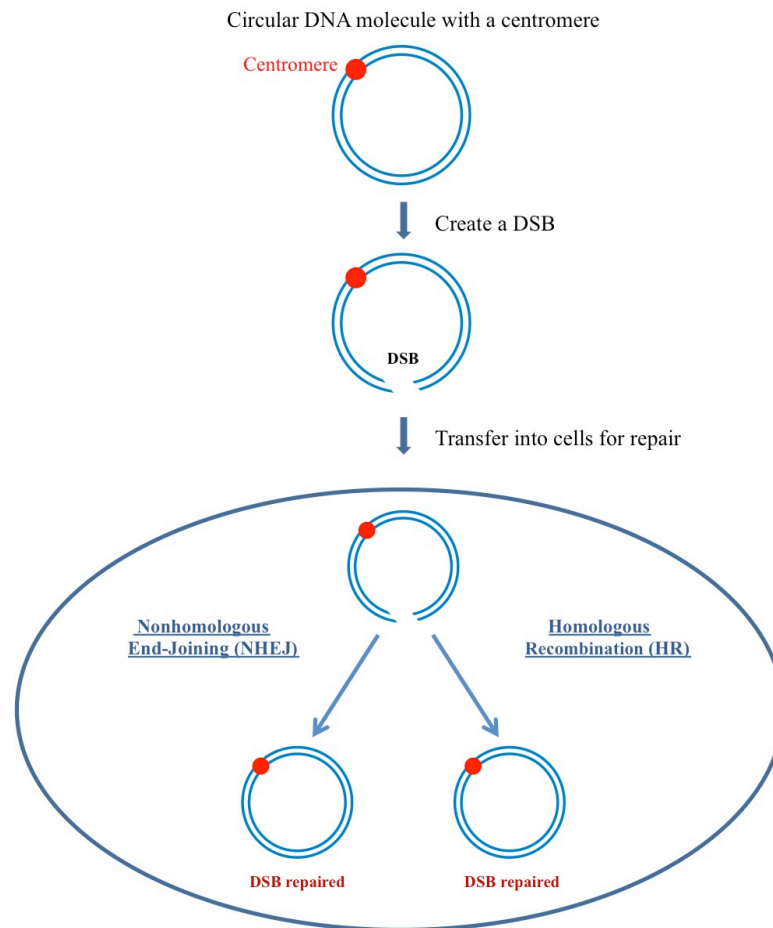


Figure 7. Plasmid DSB repair assay. A plasmid containing a DSB can in principle be repaired by either the NHEJ or the HR pathway.

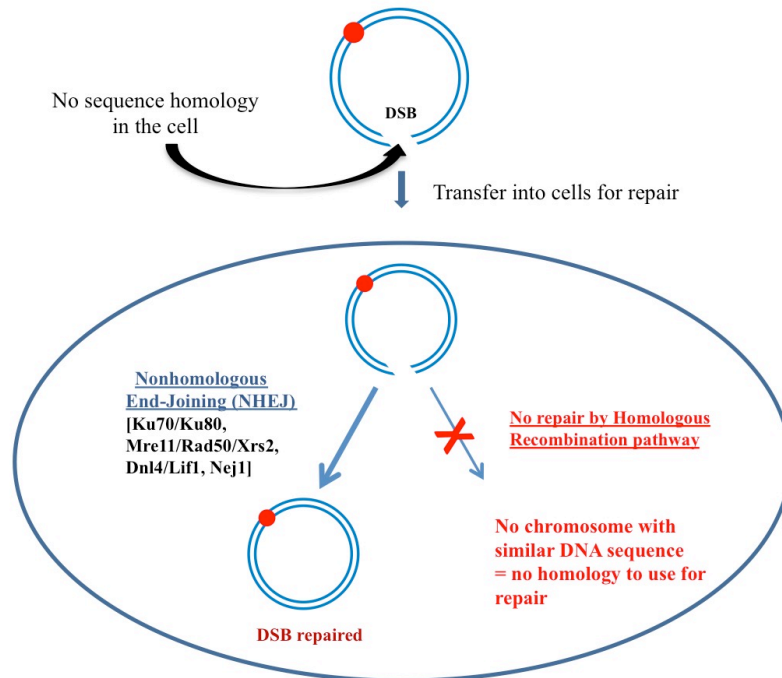


Figure 8. NHEJ DSB repair assay. Example of an assay designed specifically to measure repair by NHEJ.

Plasmid NHEJ assays are performed in this lab using the plasmid pRS315URA3 (sometimes referred to as p315URA3). This plasmid has 2 selectable markers for yeast cells, *LEU2* and *URA3*, with a unique NcoI site in the *URA3* gene (Figure 9). NcoI recognizes the 6 bp sequence 5' CCATTG 3' and digestion of pRS315URA3 creates a single DSB with 4 base overhangs.

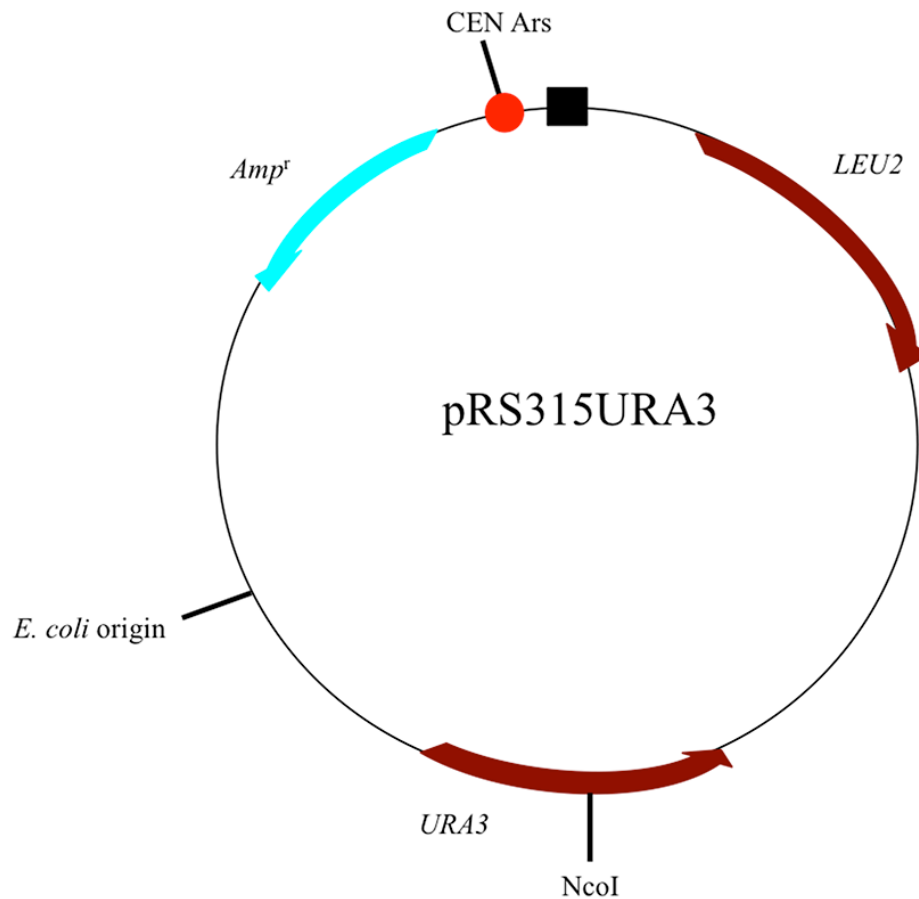


Figure 9. Plasmid map of pRS315URA3. Plasmid has a *CEN/ARS/LEU2/URA3* genotype with and *NcoI* restriction site in the *URA3* gene.

Use of the plasmid pRS315URA3 in these experiments allowed measurement of repair of a single DSB after the *NcoI*-cut DNA was transformed into yeast cells.

However, during these experiments cells were also transformed with an uncut plasmid called pRS313 that has the marker *HIS3*. DSB repair efficiencies were measured as a ratio of cut/uncut plasmids by counting colonies. What the ratio of transformed cells produced by cut/uncut plasmid illustrates is DSB repair efficiency. The ratio normalizes general transformation efficiency within the assay as well as provides indicative data pertaining to DSB repair capabilities. Cut plasmid values were acquired by spreading

onto media without leucine and uncut plasmid values from media without histidine. Two plasmids were used in the assay with one containing a gene that provides the yeast cells the capability to synthesize leucine and the other plasmid histidine. pRS313 is the uncut plasmid that contains the *HIS3* gene and pRS315URA3 (Figure 9) contains *LEU2* and the *URA3* gene that is cut by restriction endonuclease NcoI. Thus, if the cut pRS315URA3 is not repaired in the cell post-transformation, the cell will not be able to transcribe the *LEU2* gene and will be unable to grow without environmental leucine. The use of uncut pRS313 DNA acts as a baseline measurement of general transformation efficiency of the assay. This uncut value is then compared to the cut value so that true DSB repair values can be correctly obtained.

In addition to repair efficiency, DSB repair accuracy is also a concern for repair, particularly in the NHEJ pathway because NHEJ is less accurate than HR. To test accuracy, we also use the NcoI-cut pRS315URA3 plasmid. NcoI creates a DSB in the middle of the *URA3* gene. All strains from the yeast strain library are *ura3Δ* so if the pRS315URA3 plasmid is accurately repaired, then cells will grow on media without uracil. If DSB repair is accurate, then cells will be Ura⁺ and produce colonies on glucose without uracil media. If repair is inaccurate then cells will be Ura⁻ and will be unable to grow on plates without added uracil (Figure 10).

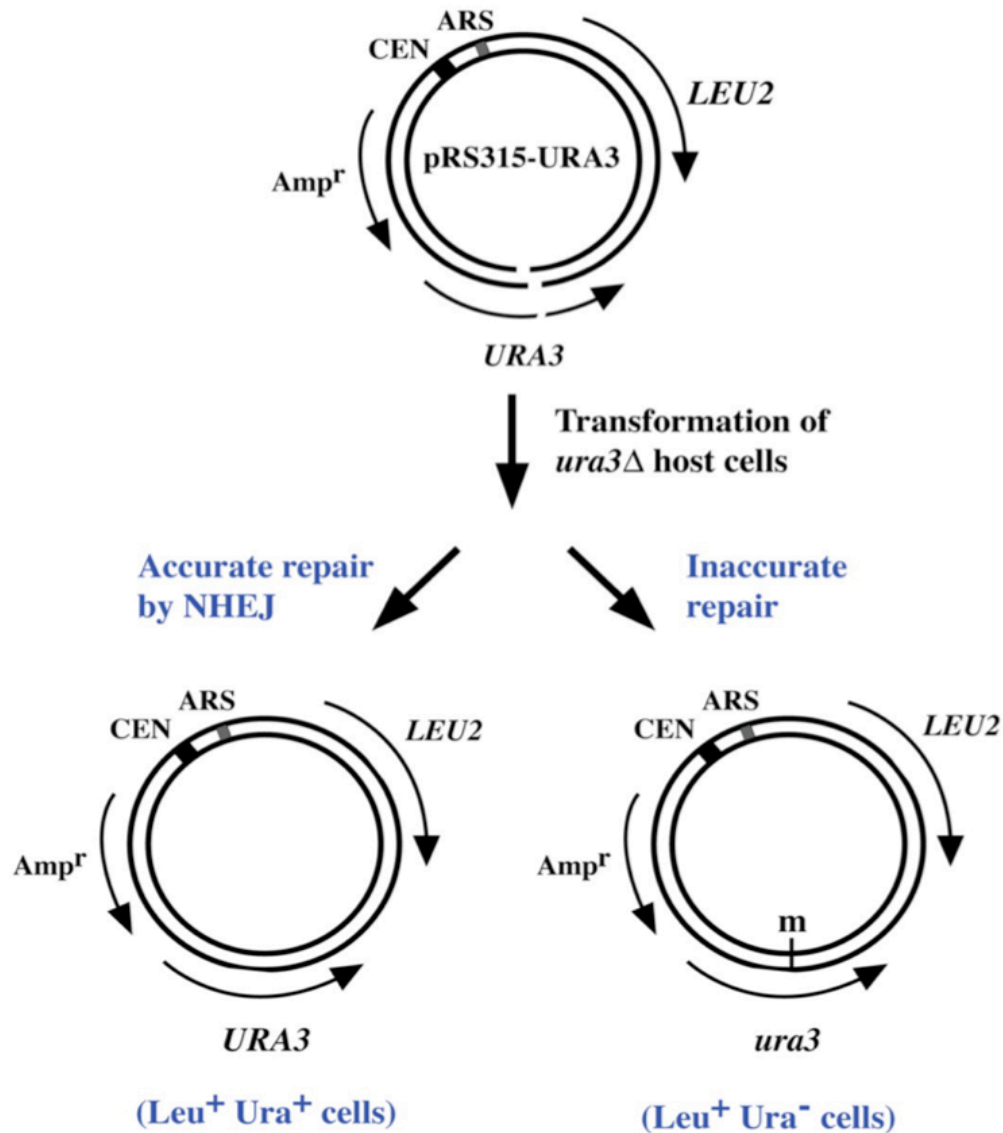


Figure 10: NHEJ DSB repair assay that permits quantitation of both the efficiency and the accuracy of repair. *NcoI*-cut *pRS315URA3* is transformed into *ura3Δ* cells and the accuracy of repair at the *URA3* gene is determined by patching *Leu⁺* cells onto glucose minus uracil media.

Using our new assay with early stationary phase cells (cultures grown overnight in YPDA broth), NHEJ efficiencies of cells containing mutations in most known NHEJ pathway genes were measured. These studies were initiated in our lab by graduate student

Whitney Wood, who did several preliminary tests with known NHEJ and HR mutants using cells of the BY4742 background (59). Four or five assays were done for each strain and the results were averaged. The experiments revealed strong defects in repair efficiencies in each of the NHEJ mutants but not in the HR-deficient strains.

Interestingly, initial studies repeatedly yielded different levels of DSB repair efficiency among known NHEJ mutants. For example, repair was severely decreased in mutants of the Ku complex (inactivation of *YKU70* or *YKU80*) or DNA ligase IV complex (inactivation of *LIF1* or *DNL4*) with reduction from 614 to 994 fold relative to WT cells (Table 2). In contrast, inactivation of two genes encoding subunits from the Mrx complex (*RAD50* and *MRE11*) produced only small reductions ranging from 6-8 fold. Additionally, deletion of *NEJ1*, which encodes the third subunit of the Dnl4-Lif1-Nej1 DNA ligase IV complex, consistently reduced efficiency by only ~200 fold versus the > 600 fold reductions seen in *dnl4* and *lif1* mutants.

All the experiments were done using haploid *MAT α* strains; however, to test the reproducibility of the *nej1* results, a *MAT α* strain was also assayed. The *MAT α nej1* mutant showed a reduction of 212 fold, which was similar to the 245 fold reduction seen in the *MAT α nej1* strain. Two other mutants, *sir2* and *sir4*, were also tested. Inactivation of these genes strongly reduces transcription of the *NEJ1* gene, producing cells that are effectively *nej1⁻*. NHEJ was reduced by ~50 fold in each of the *sir* strains, which is much less than that seen in the *yku* or *dnl4* mutants and more similar to that seen in the *nej1* deletion strains. Finally, two mutants defective in homologous recombination, *rad52* and *rad54*, were tested and found to be capable of NHEJ repair at approximately WT levels

(Table 2). The differentiation of DSB repair efficiencies indicate that each protein complex and subunit of that complex in the NHEJ pathway vary in level of importance.

Table 2. DSB repair efficiencies determined using the new early stationary phase cell method.

Strain	Function of Protein	Normalized Repair Efficiency	Fold Change
WT	N/A	100% \pm 16.5%	N/A
<i>yku70</i>	protects ends, recruit MRX	0.16% \pm 0.06%	-625
<i>yku80</i>	“ ”	0.16% \pm 0.05%	-625
<i>mre11</i>	tethers ends, ensures proximity	13.2% \pm 5.3%	-7.6
<i>rad50</i>	“ ”	16.8% \pm 1.7%	-6.0
<i>lif1</i>	ligates ends together	0.10% \pm 0.02%	-994
<i>dnl4</i>	“ ”	0.13% \pm 0.04%	-769
<i>nej1 (MATα)</i>	ligation and Yku binding	0.41% \pm 0.11%	-244
<i>nej1 (MATα)</i>	“ ”	0.47% \pm 0.05%	-213
<i>sir2</i>	regulate expression of <i>NEJ1</i>	2.20% \pm 0.59%	-45
<i>sir4</i>	“ ”	2.20% \pm 0.26%	-45
<i>rad52</i>	homologous recombination	94.9% \pm 12.3%	-1.0
<i>rad54</i>	“ ”	110.1% \pm 22.3%	+0.9

The same known repair mutants that were tested for repair efficiency in Table 2 were also tested for repair accuracy. Yku and DNA ligase IV complex mutants exhibited large decreases in accuracy with Ura^r error frequencies ranging from 30% to 73% versus only 1% for WT cells. In contrast, Mrx complex mutants did not demonstrate a decrease in DSB repair accuracy that deviated far from WT (Table 3). The Mrx complex is what tethers the broken ends together after binding to each side of the DSB. Though repair efficiency was decreased in Mrx mutants, the *mre11* and *rad50* strains exhibited accurate repair. Thus the Mrx complex is not necessary to ensure accurate repair. If a cell can

repair the DSB in *mre11* and *rad50* mutants, they do so accurately. *yku* mutants had an error frequency of 30-41% and DNA ligase IV mutants 64-73%. The accuracy testing indicates that, in the absence of the Yku and DNA ligase IV complexes, recombination-independent repair of DSBs is highly inaccurate.

Table 3. Established NHEJ mutant effects on DSB repair accuracy.

Strain	Function of Protein	Ura ⁻ /Leu ⁺	Error Frequency
WT	N/A	4/400	1%
<i>yku70</i>	protects ends, recruit Mrx	30/100	30%
<i>yku80</i>	“ ”	41/100	41%
<i>mre11</i>	tethers ends, ensures proximity	0/100	0%
<i>rad50</i>	“ ”	0/100	0%
<i>lif1</i>	ligates ends together	64/100	64%
<i>dnl4</i>	“ ”	73/100	73%
<i>nej1 (MAT α)</i>	ligation and Yku binding	7/100	7%
<i>nej1 (MAT a)</i>	“ ”	4/100	4%
<i>sir2</i>	regulate expression of <i>NEJ1</i>	4/100	4%
<i>sir4</i>	“ ”	0/100	0%
<i>rad52</i>	homologous recombination	1/100	1%
<i>rad54</i>	“ ”	0/100	0%

According to Table 2 and Table 3, the Mrx complex does not appear to be as significant as previously thought. A possible reason for this is due to the nature of the assays used. Experiments were designed with a DSB on plasmid DNA, rather than chromosomal DNA. If the Mrx complex is what tethers the broken DNA together, ensuring that the DNA strands do not migrate too far away, using a plasmid DNA already partially prevents this from happening. A DSB on plasmid DNA (of ~5,000 bp) only creates one linear piece of DNA and these broken ends cannot wander too far away

anyway. A DSB on chromosomal DNA, on the other hand, creates two separate linear pieces. Chromosomal DNA is much larger and has a higher chance of distancing itself because they two ends are not intrinsically linked together. Therefore, if we were to test the efficiency and accuracy of NHEJ repair on chromosomal DNA, perhaps the Mrx complex would prove to be more necessary.

In addition to the data analysis shown in Tables 2 and 3, a literature review of plasmid NHEJ efficiency from 1996 to 2012 was conducted for the current project. The results illustrate the intensive investigative efforts of DSB repair research (Table 4). *yku70*, *yku80*, *mre11*, *rad50*, *nej1*, *lif1*, *dnl4*, *rad50*, and *rad52* group mutants were repeatedly tested for DSB repair efficiency. Known NHEJ and HR mutants that were tested are shown in the right side of the table with fold change in repair shown in parentheses. Some of the numbers were estimated from visual analysis of graphs and were therefore approximations. Several studies tested multiple genes from the different NHEJ protein complexes in the same study such as Boulton and Jackson (1996), Milne *et al.* (1996), Tsukamoto *et al.* (1997) Schar *et al.* (1997), Lee *et al.* (1999), Ooi *et al.* (2001), Valencia *et al.* (2001), Karathanasis and Wilson (2002), Daley and Wilson (2005), Lewis *et al.* (2005), Palmboos *et al.* (2008), Chen and Tomkinson (2010), and Bahmed *et al.* (2010) (21, 22, 23, 24, 25, 26, 27, 29, 32, 36, 39, 45, 48, 51).

Table 4. Literature review of plasmid NHEJ efficiency.

Paper	Paper (Year)	Mutants (Fold Decrease)
Boulton and Jackson	Nucleic Acids Res. (1996)	<i>yku70</i> (23), <i>yku80</i> (27), <i>rad52</i> (2)
Boulton and Jackson	EMBO (1996)	<i>yku70</i> (12), <i>rad52</i> (2)
Milne <i>et al.</i>	Mol. and Cell Biol. (1996)	<i>yku70</i> (14), <i>yku80</i> (10), <i>rad50</i> (12), <i>rad52</i> (3)
Tsukamoto <i>et al.</i>	Nature Letters (1997)	<i>yku70</i> (20), <i>sir2</i> (20), <i>sir3</i> (20), <i>sir4</i> (20)
Schar <i>et al.</i>	Genes and Devel. (1997)	<i>dnl4</i> (200), <i>rad52</i> (1)
Lee <i>et al.</i>	Current Biol. (1999)	<i>yku70</i> (20), <i>sir2</i> (10), <i>sir3</i> (8), <i>sir4</i> (4)
Ooi <i>et al.</i>	Science (2001)	<i>yku80</i> (117), <i>dnl4</i> (470), <i>nej1</i> (235)
Lewis <i>et al.</i>	Genetics (2001)	<i>rad50</i> (50), <i>mre11</i> (50)
Valencia <i>et al.</i>	Nature Letters (2001)	<i>yku70</i> (20), <i>nej1</i> (40), <i>sir2</i> (10)
Kegel <i>et al.</i>	Current Biol. (2001)	<i>dnl4</i> (12), <i>nej1</i> (7)
Erdemir <i>et al.</i>	Mol. Microbiol. (2002)	<i>yku70</i> (4)
Karathanasis and Wilson	Genetics (2002)	<i>yku70</i> (18), <i>dnl4</i> (18), <i>rad52</i> (1)
Lewis <i>et al.</i>	Genetics (2004)	<i>mre11</i> (21)
Jazayeri <i>et al.</i>	PNAS (2004)	<i>yku80</i> (18)
Schar <i>et al.</i>	Nucleic Acids Res. (2004)	<i>dnl4</i> (154), <i>rad52</i> (4)
Daley and Wilson	Mol. and Cell Bio. (2004)	<i>yku70</i> (1), <i>dnl4</i> (1), <i>rad52</i> (7)
Virgilio and Gautier	JCB (2005)	<i>mre11</i> (1)
Zhang and Paull	DNA Repair (2005)	<i>mre11</i> (2)
Lewis <i>et al.</i>	Nucleic Acids Res. (2005)	<i>yku70</i> (19), <i>rad50</i> (15)
Shim <i>et al.</i>	Mol. and Cell Biol. (2005)	<i>yku70</i> (~40)
Bilsland <i>et al.</i>	DNA Rep. (2007)	<i>yku80</i> (10)
Herrmann <i>et al.</i>	Nucleic Acids Res. (2007)	<i>dnl4</i> (67.5)
Jessulat <i>et al.</i>	ABB (2008)	<i>yku70</i> (77)
Pitre <i>et al.</i>	Nucleic Acids Res. (2008)	<i>yku80</i> (25)
Palmbos <i>et al.</i>	Genetics (2008)	<i>lif1</i> (5), <i>xrs2</i> (45)
Carter <i>et al.</i>	PNAS (2009)	<i>nej1</i> (1), <i>rad52</i> (20)
Bahmed <i>et al.</i>	PNAS (2010)	<i>yku70</i> (14), <i>dnl4</i> (30), <i>rad52</i> (3)
Chen and Tomkinson	J. Biol. Chem. (2010)	<i>lif1</i> (20), <i>nej1</i> (20)
Tao <i>et al.</i>	Cell Res. (2011)	<i>yku70</i> (25)
Hohl <i>et al.</i>	Nature Struct. and Mol. Biol. (2011)	<i>rad50</i> (17)
Bahmed <i>et al.</i>	Nucleic Acids Res. (2011)	<i>yku80</i> (10)
Srividya <i>et al.</i>	PlosOne (2012)	<i>yku70</i> (24)
Matsuzaki <i>et al.</i>	Genes-to-Cells (2012)	<i>lif1</i> (> 100)

Summarizing the results of the past research listed in Table 4 shows a relatively narrow fold reduction among known NHEJ mutants (Table 5). Median reduction in plasmid NHEJ repair for the 8 major NHEJ mutants (*yku70*, *yku80*, *dnl4*, *lif1*, *nej1*, *rad50*, *mre11*, and, *xrs2*) all ranged from 11.5-20.0 fold. In addition, no clear differences

were detected between the 3 complexes: *yku* mutants, *mrx* mutants, and DNA ligase IV mutants were all similar. These numbers are in stark contrast to the values obtained in the lab using the new transformation assay (Table 2) which produced reductions of >600 fold in *yku70*, *yku80*, *dnl4* and *lif1* mutants and much smaller reductions in the other strains. The conclusion that the new assay was an improvement is also supported by results obtained in several of the past studies that tested multiple NHEJ mutants at the same time, e.g., *yku70* vs. *rad50* mutants (22, 39) and *nej1* vs. *dnl4* or *yku* mutants (27, 29, 30, 48) (See Table 4).

Table 5. Summary of NHEJ mutant efficiency from past literature.

No. Published Studies	Strain	Median	Mean	Range
14	<i>yku70</i>	20	22.1	1-77
7	<i>yku80</i>	18.0	31.0	10-117
4	<i>mre11</i>	11.5	18.5	1-50
3	<i>rad50</i>	16.0	23.6	12-50
1	<i>xrs2</i>	N/A	45	N/A
3	<i>lif1</i>	20.0	41.7	5-100
8	<i>dnl4</i>	20.0	106.3	1-470
5	<i>nej1</i>	20.0	60.7	1-235
3	<i>sir2</i>	10.0	13.3	10-20
2	<i>sir3</i>	13.8	13.8	7.5-20
2	<i>sir4</i>	12.0	12.0	4-20
8	<i>rad52</i>	3.00	4.78	1-20

With the new ability to further differentiate the degree of importance of these known NHEJ mutants, investigation of the 71 EcoRI^s mutants using this assay can effectively screen NHEJ capabilities for both DSB repair efficiency and accuracy. Because of the chemical assault yeast cells endure during our improved transformation

protocol, we assumed there may be a need for a recovery period in rich YPDA broth. The efficacy of this step was tested by comparing repair efficiencies between growout with rich broth and no grow out. BY4742 and BY4741 cells were grown in duplicate and transformed either with or without a YPDA growout period shaking at 30° C for 30 minutes. The average ratio of cut/uncut plasmid DNA transformation efficiency in Table 2 is a combination of BY4742 (*MAT α*) and BY4741 (*MATa*). There is, however, no benefit to using a rich broth incubatory period for determining NHEJ DSB repair. The experiment comparing DSB repair efficiency with grow-out vs non-grow-out periods in rich broth showed no significant difference (Table 6).

Table 6. DSB repair efficiencies of WT cells. Comparing average ratio of transformation efficiency of cut plasmid/uncut plasmid in WT cells.

	Average Ratio	SD
No grow out	1.7	0
Grow out	1.8	+ 0.07

Given the large fold decrease in NHEJ repair efficiency seen in *dnl4* cells, it was chosen for use as a negative control when testing EcoRI^S mutants. Before screening of the 73 EcoRI^S mutants, *dnl4* and *rad50* cells were tested for NHEJ DSB repair efficiency. Initially, tests revealed that the fold reduction of *dnl4* mutants were up to 1100x fold, though there was some variability. Because each test is internally controlled, the variability seen in *dnl4* strains, the negative control, is not an issue when pertaining to the investigation of other mutants and their capacity to repair DSBs.

Seventy-three new EcoRI^S mutants were recently identified (13) and tested for DSB repair efficiency in the current study (Table 7). Their identification was a

continuation of work done by Bennett *et al.* and Game *et al.* which identified over 200 gamma radiation sensitive mutants (69, 70). The McKinney *et al.* study identified 73 EcoRI^S mutants, most of which have not been previously linked to DSB repair. All 73 mutants are sensitive to *in vivo* expression of EcoRI endonuclease using the *GALI* promoter system and many of them are also sensitive to the DSB-inducing chemicals MMS and bleomycin.

Table 7. Seventy-three new EcoRI-sensitive mutants identified by library screening.

Function	Genes
Sister chromatid cohesion	<i>ctf4, ctf8, dcc1, htl1</i>
Histone modification/remodeling	<i>arp5, eaf1, gcn5, rtt109(rem50), spt10, ubp8</i>
Nuclease processing of DNA	<i>exo1, mms4, sae2, ylr235c/top3^a</i>
Chromosome stability/segregation	<i>bik1, cgi121, cnm67, ddc1, mms22</i>
Transcription regulation	<i>apq13/net1^a, bud32, bur2, ccr4, not5, nup84, rpb9, bud30/rpc53^a, rtf1, sfp1, spt20, taf14, ume6, yml009w-b/spt5^a</i>
RNA processing/modification	<i>cdc40, lrp1, lsm7, trm9, tsr2/ylr434c^a, ydr433w/np13^a</i>
Protein posttranslational modification	<i>akr1, bck1, cax4, mms2, och1, rad5, ubr1, yml012c-a/ubx2^a</i>
Cell membrane/cell wall	<i>cis3, hsp150, rvs161, sam37, vma7, vph2/ykl118w^a</i>
Mitochondrial proteins	<i>atp2, img2, mct1, ygl218w/mdm34^a, mrps35, rsm7/yjr114w^a, sco1</i>
Other / Unknown	<i>adk1, ado1, bud19/rpl39, gnd1/yhr182c-a, ids2, lip5, och1, psy1/ykl075c, rpl31a, slm4, srv2, ybr099c-1, ydr417c/rpl12b, ynr068c</i>

^a Names separated by a forward slash indicate loci where the deletion-disruption performed in the construction of the library strain affected two overlapping open reading frames. Functions are described for the verified gene only. Source: The Saccharomyces Genome Database (www.yeastgenome.org)

Overnight cultures were prepared in YPDA broth in groups of three for each mutant, with *dnl4* and WT cells being the negative and positive controls, respectively. Cells were transformed with NcoI-cut pRS315URA3 and pRS313 as described in Chapter 2. Mutants with ≥ 3 fold difference in repair efficiency relative to WT cells were re-tested to confirm that the defect was reproducible. The mutants surviving these two tests were then re-tested using new versions of the mutants of the opposite mating type. Later tests employed more isolates in each assay for better statistics.

Midipreps of plasmids were prepared by rapid alkaline lysis. Plasmid DNAs were harvested from *E. coli*, chemically extracted using Tris/EDTA, SDS/NaOH, and KOAc solutions, then ethanol precipitated. pRS315URA3 plasmids were then digested with restriction endonuclease NcoI. Proper plasmid digestion was confirmed by gel electrophoresis (Figure 11).

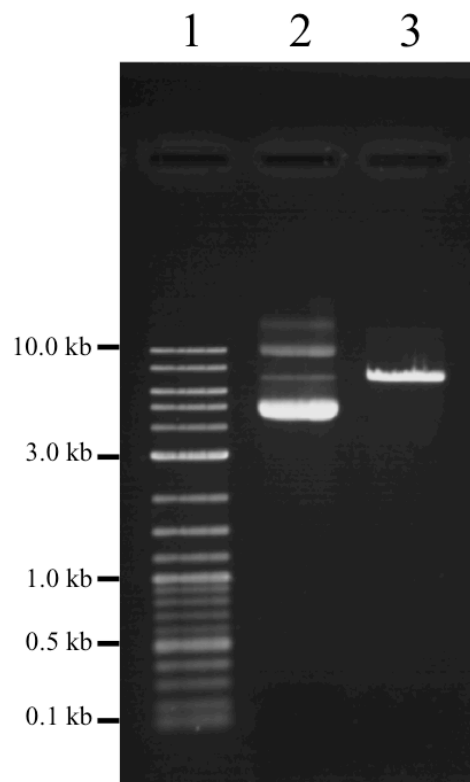


Figure 11. Agarose gel electrophoresis of pRS315URA cut with NcoI. Lane 1. 2-Log DNA ladder. Lane 2. undigested pRS315URA3. Lane 3. NcoI cut pRS315URA3.

The first screening of the 73 EcoRI^S mutants using our improved transformation method yielded 18 mutant strains that exhibited a DSB repair efficiency change relative to WT of at least 3 fold. Results are shown in Table 8 and Table 9, where mutant strains were categorized into known cellular function, nuclear and non-nuclear/unknown, respectively. From Table 8, genes encoding proteins related to sister chromatid cohesion, histone modification/remodeling, chromosome stability/segregation, transcription regulation, and RNA processing/modification showed reduced NHEJ repair. Repair genes encoding nonnuclear proteins included protein posttranslational modification, cell membrane/cell wall, mitochondrial proteins, and “other” (Table 9). Interestingly, DSB repair efficiencies were increased in two mutant strains, *atp2* and *srv2*. *ATP2* codes for

the beta subunit of mitochondrial F1F0 ATP synthase (71). *SRV2* is a cyclase-associated protein that binds to adenylate cyclase assisting activation by RAS, a signaling GTPase (72).

Table 8. Results form first round of NHEJ efficiency testing for genes encoding proteins with nuclear functions^a.

Strain	Fold Change from WT	Strain	Fold Change from WT
<u>Sister Chromatid Cohesion</u>		<u>Transcription Regulation</u>	
<i>ctf4</i>	-1.15x	<i>apq13/net1</i>	-1.77x
<i>ctf8</i>	-1.23x	<i>bud32</i>	-16.5x
<i>dcc1</i>	-1.17x	<i>bur2</i>	-1.11x
<i>htl1</i>	-8.32x	<i>ccr4</i>	-0.63x
		<i>not5</i>	-0.67x
		<i>nup84</i>	-1.00x
<u>Histone Modification/Remodeling</u>			
<i>arp5</i>	-6.75x	<i>rpb9</i>	-3.01x
<i>eaf1/opi7</i>	-1.78x	<i>bud30/rpc53</i>	-0.48x
<i>gcn5</i>	-1.38x	<i>rtf1</i>	-1.66x
<i>spt10</i>	-5.45x	<i>spt20</i>	-1.1x
<i>ubp8</i>	-1.06x	<i>taf14</i>	-5.76x
<i>rtt109 (rem50)</i>	-1.75x	<i>ume6</i>	-1.80x
		<i>yml009w-b/spt5</i>	-0.66x
		<i>sfp1</i>	-2.23x
<u>Nuclease Processing of DNA</u>			
<i>exo1</i>	-1.00x	<u>RNA processing/modification</u>	
<i>mms4/ybr099c</i>	-1.60x	<i>cdc40</i>	-1.02x
<i>sae2</i>	-1.02x	<i>lrp1</i>	-1.65x
<i>ylr235c/top3</i>	-1.89x	<i>lsm7</i>	-2.94x
		<i>trm9</i>	-0.66x
<u>Chromosome Stability/Segregation</u>			
<i>bik1</i>	-2.23x	<i>tsr2/ylr434c</i>	-4.70x
<i>cgi121</i>	-0.74x	<i>npl3/ydr433</i>	-1.63x
<i>cnm67</i>	-3.39x		
<i>ddc1</i>	-1.48x		
<i>mms22</i>	-3.55x		

^a Mutants shown in boldface displayed a change of ≥ 3 fold

Table 9. Results from first round of NHEJ efficiency testing for genes encoding proteins with non-nuclear or unknown functions^a.

Strain	Fold Change from WT	Strain	Fold Change from WT
<u>Protein Posttranslational Modification</u>		<u>Other</u>	
<i>akr1</i>	-1.84x	<i>ydr417c/rpl12b</i>	-0.48x
<i>bck1</i>	-1.49x	<i>srv2</i>	+3.13x
<i>cax4</i>	-1.69x	<i>adol</i>	-0.84x
<i>mms2</i>	-1.53x	<i>lip5</i>	-23.00x
<i>och1</i>	-0.79x	<i>ids2</i>	-0.83x
<i>rad5</i>	-0.59x	<i>bud19/rpl39</i>	-1.18x
<i>ubr1</i>	-3.16x	<i>ybr099c-1</i>	-1.70x
<i>ubx2/yml012c-a</i>	-1.40x	<i>och1</i>	-0.79x
		<i>psy1/ykl075c</i>	-1.18x
<u>Cell Membrane/Cell Wall</u>		<i>rpl31a</i>	-0.76x
<i>cis3</i>	-0.88x	<i>ynr068c</i>	-1.18x
<i>hsp150</i>	-0.48x	<i>adk1</i>	-53.42x
<i>rvs161</i>	-1.16x	<i>gnd1/yhr182c-a</i>	-0.65x
<i>sam37</i>	-1.00x	<i>slm4</i>	-0.57x
<i>vma7</i>	-3.88x		
<i>vph2/ykl118w</i>	-9.67x		
<u>Mitochondrial Proteins</u>			
<i>atp2</i>	+3.57x		
<i>img2</i>	-2.87x		
<i>mct1</i>	-13.00x		
<i>ygl218w/mdm34</i>	-0.48		
<i>mrps35</i>	-0.70		
<i>rsm7/yjr114w</i>	-1.53x		
<i>sco1</i>	-4.23x		

^a Mutants shown in boldface displayed a change of ≥ 3 fold

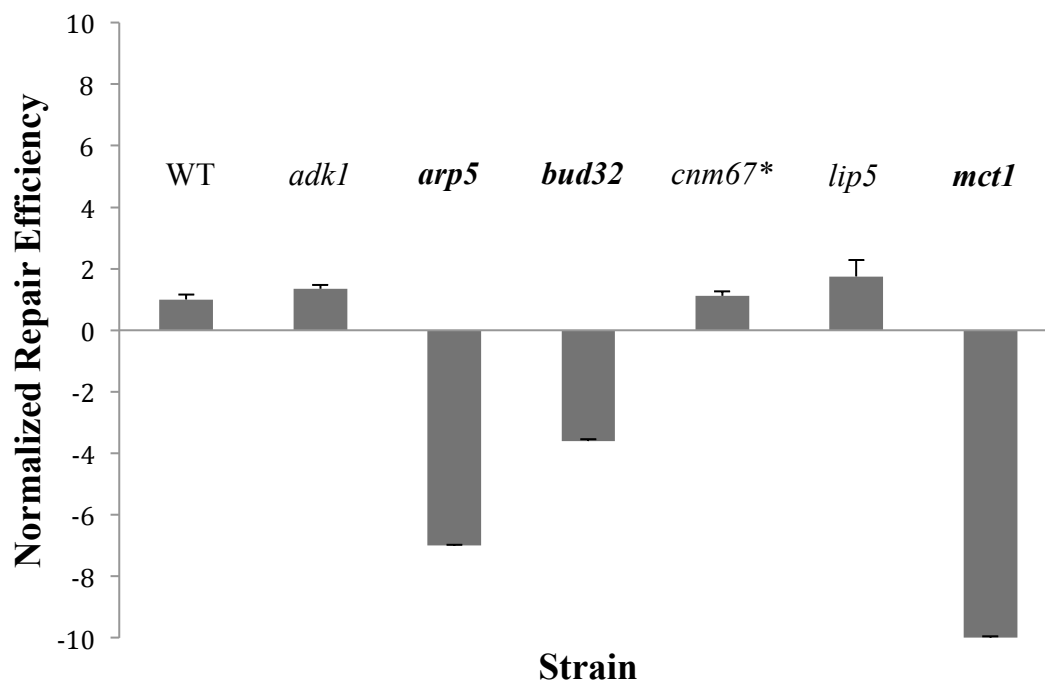
All mutant strains whose NHEJ repair efficiency was significantly increased/reduced by at least 3 fold were tested again to ensure reproducibility. Six mutant strains showed significant changes in DSB repair efficiency in the second trial (Table 10), shown in boldface. All changes were of reduction in performance, rather than an increase. Three mutants were strains lacking genes associated with nuclear functions and three for non-nuclear functions. Histone modification/remodeling, chromosome stability/segregation, and transcription regulation each had one strain with reduced DSB repair performance. For outer nuclear functions, one mitochondrial protein and two “other” gene mutants were reduced in DSB repair efficiency.

Table 10. Mutant results of re-testing with reduction in DSB repair efficiency from first round of NHEJ testing.

Mutant	1st Test	2nd Test	
	Fold Change	%WT ^a	Fold Change
WT	N/A	100% ± 15.6%	N/A
<i>bud32</i>	-16.5x	25.0% ± 2.8%	-4.00x
<i>cnm67</i>	-3.39x	20.9% ± 1.5%	-4.78x
<i>htl1</i>	-8.32x	41.6% ± 10.8%	-2.40x
<i>srv2</i>	+3.13x	107.8% ± 20.8%	+1.09x
<i>lip5</i>	-23.0x	6.25% ± 0.8%	-16.00x
<i>ubr1</i>	-3.16	123.3 ± 12.8%	+1.23x
<i>tsr2/ylr434c</i>	-4.70x	88.4% ± 22.1%	-1.13x
<i>rpb9</i>	-3.01x	88.9% ± 21.2%	-1.12x
<i>spt10</i>	-5.45x	62.5% ± 19.4%	-1.60x
<i>arp5</i>	-6.75x	12.3% ± 7.1%	-8.11x
<i>taf14</i>	-5.76x	69.1% ± 32.3%	-1.45x
<i>mms22</i>	-3.55x	105.5% ± 9.4%	+1.05x
<i>mct1</i>	-13.0x	4.7% ± 1.0%	-21.33x
<i>vph2/ykl118w</i>	-9.67x	133.6% ± 21.8%	+1.33x
<i>adk1</i>	-53.4x	7.50% ± 1.7%	-13.33x
<i>sco1</i>	-4.23x	41.4% ± 5.5%	-2.42x
<i>vma7</i>	-3.88x	96.9% ± 16.6%	-1.03x
<i>atp2</i>	+3.57x	270.0% ± 130.0%	+2.70x

^aAverage repair efficiency relative to WT cells

The strains that were significantly decreased in NHEJ repair efficiency were tested a third time but using haploid strains of the opposite mating type. The rationale for this was to eliminate the possibility that the library mutant strains were constructed accidentally with a second mutation unbeknownst to the researchers. If the deficiency in repair is because of an unknown second mutation, this would not provide concrete evidence for said library mutant's DSB repair capabilities. Thus, all 6 mutants were tested for a third time with the opposite mating type (a or α). Only half of the mutants displayed a significant fold change in NHEJ repair; all were reductions in repair efficiency (Figure 12). Two mutants were for genes coding for nuclear functions, *bud32* and *arp5*, and one for mitochondrial function, *mct1*.



**cnm67* mutants were not tested a third time by using the opposite haploid strain but, rather, by a knock-out mutant created in our lab. This *cnm67* strain was tested twice to ensure reproducibility.

Figure 12. NHEJ efficiencies of mutants tested using opposite mating type strains. Mutants in bold are those which exhibited significant decrease in repair efficiency. WT cells have repair efficiency at 1.0 ± 0.15 . *arp5* had repair average of 0.14 ± 0.03 , *bud32* at 0.30 ± 0.06 , and *mct1* at 0.10 ± 0.05 .

Bud32 is a protein kinase involved in transcriptional regulation through tRNA modification with the KEOPS/EKC complex (73). Bud32, however, does not behave like a kinase in this complex, but rather acts as a P-loop ATPase that dissociates tRNA. Further studies provide implications that Bud32 is required for telomere capping, length regulation, and recombination via the KEOPS complex (74, 75). NHEJ repair efficiency was reduced by 3.6 fold in the three tests of *bud32* cells. This reduction range is similar to that of *mre11* mutants that we have found in our lab. Perhaps Bud32 is a protein that is important for DSB repair, like Mre11, through transcriptional regulation of NHEJ

complex proteins, or another function of the KEOPS/EKC complex still unknown to researchers.

Arp5, an actin-related protein, is another nuclear protein that plays a role in histone remodeling as a part of the Ino80 complex. Without Arp5, ATPase activity of the Ino80 complex is compromised and this function may be required for physical interfacing with histone proteins (76). Arp5 primarily interacts with the +1 nucleosome region which, according to Yen *et al.*, may be the gateway to transcription (77). Our studies reveal that *arp5* cells have 6-8x reduction in NHEJ repair. Again, this is similar to the lower limits of *mre11* and *rad50* fold reduction in repair efficiency. Like *bud32* cells, it is conceivable that Arp5 acts indirectly by affecting transcription of NHEJ complex genes through histone modification. Alternatively, Arp5 may be involved in remodeling or shifting the positions of histones to allow access for DNA repair enzymes.

Whereas Bud32 and Arp5 function in the nucleus, Mct1 is a mitochondrial protein. Mct1, malonyl-CoA:ACP transferase, is a putative element in type II mitochondrial fatty acid synthesis (78). Mutant studies found *mct1* cells have markedly reduced respiration, existing in an entirely fermentive state, and have underdeveloped mitochondria. Though mitochondrial fatty acid synthesis (FAS) appears to be unrelated to nuclear functionality or even DNA repair, a study by Hiltunen *et al.* suggested that type II mitochondrial FAS has an impact on mitochondrial RNA metabolism (79).

Investigation of DSB repair efficacy through the homologous recombination (HR) pathway on 48 of the 73 mutants that are EcoRI^S was completed by previous graduate student Brian Sanderson (80). The 48 proteins are known to be involved in nuclear functions. Plasmid:chromosome recombination assays revealed that *bud32* mutants

exhibited a 10 fold increase in this type of DSB repair relative to WT cells. *arp5* mutants did not express a significant fold change in recombination relative to WT and Mct1 is not a nuclear protein so it was not tested.

NHEJ is a more error prone process than homologous recombination. This error rate is known to be increased in some NHEJ mutants (39, 47, 51, 81, 82). Therefore, accuracy testing was also performed with each of the 73 EcoRI^S mutants. Table 11 provides a listing of accuracy results for all nuclear functioning genes for the first trial. Like with efficiency testing, multiple experiments were performed with each mutant to identify those that consistently exhibited higher levels of Ura⁻ Leu⁺ cells than WT. For most of the mutants, 100 Leu⁺ transformants were screened to determine the frequency of inaccurate repair. *rtt109*, *mms22*, *rtf1*, *spt20*, and *lsm7* all had error frequencies of $\geq 5\%$. Relative to WT cells, which had an error frequency of 0.5-1.0%, this was a 10 fold or higher increase. These mutants were from the following categories: histone modification/remodeling, chromosome stability/segregation, transcription regulation, and RNA processing/modification.

Table 12 displays the accuracy results for proteins known to function outside the nucleus or whose locations are not known. First trial testing produced three mutants with an error frequency of 5% or higher in the mitochondrial proteins and “other” category. *atp2*, *mct1*, *rsm7/yjr114w*, *lip5*, *ask1*, and, *gnd1/yhr182c-a* mutants all displayed $\geq 5\%$ Ura⁻ cells among the cells transformed with NcoI-cut pRS315URA3.

Table 11. Results from first round of NHEJ accuracy testing for genes encoding proteins with nuclear functions.

Strain	Ura⁻/Leu⁺	%
<u>Sister Chromatid Cohesion</u>		
<i>ctf4</i>	3/100	3%
<i>ctf8</i>	0/100	0%
<i>dcc1</i>	1/100	1%
<i>htl1</i>	0/73	0%
<u>Histone Modification/Remodeling</u>		
<i>arp5</i>	0/50	0%
<i>eaf1/opi7</i>	0/100	0%
<i>gcn5</i>	0/100	0%
<i>spt10</i>	1/27	3%
<i>ubp8</i>	3/200	1.5%
<i>rtt109 (rem50)</i>	3/40	7.5%
<u>Nuclease Processing of DNA</u>		
<i>exo1</i>	1/100	1%
<i>mms4/ybr099c</i>	2/100	2%
<i>sae2</i>	0/100	0%
<i>ylr235c/top3</i>	0/38	0%
<u>Chromosome Stability/Segregation</u>		
<i>bik1</i>	3/100	3%
<i>cgi121</i>	1/100	1%
<i>cnm67</i>	0/21	0%
<i>ddc1</i>	0/100	0%
<i>mms22</i>	15/100	15%
<u>Transcription Regulation</u>		
<i>apq13/net1</i>	2/100	2%
<i>bud32</i>	0/14	0%
<i>bur2</i>	3/100	3%
<i>ccr4</i>	0/100	0)
<i>not5</i>	1/100	1%
<i>nup84</i>	0/100	0%
<i>rpb9</i>	1/100	1%
<i>bud30/rpc53</i>	0/100	0%
<i>rtf1</i>	7/100	7%
<i>spt20</i>	11/100	11%
<i>taf14</i>	1/100	1%
<i>ume6</i>	4/100	4%
<i>yml009w-b/spt5</i>	1/100	1%
<i>sfp1</i>	1/36	2.7%
<u>RNA processing/modification</u>		
<i>cdc40</i>	2/100	2%
<i>lrp1</i>	1/100	1%
<i>lsm7</i>	14/100	14%
<i>trm9</i>	1/100	1%
<i>tsr2/ylr434c</i>	0/20	0%
<i>np13/ydr433</i>	0/100	0%

Table 12. Results from first round of NHEJ accuracy testing for genes encoding proteins with non-nuclear or unknown functions.

Strain	Ura⁻/Leu⁺	%
<u>Protein Posttranslational Modification</u>		
<i>akr1</i>	2/100	2%
<i>bck1</i>	1/100	1%
<i>cax4</i>	0/89	0%
<i>mms2</i>	0/100	0%
<i>och1</i>	1/100	1%
<i>rad5</i>	2/100	2%
<i>ubr1</i>	3/100	3%
<i>ubx2/yml1012c-a</i>	0/100	0%
<u>Cell Membrane/Cell Wall</u>		
<i>cis3</i>	0/100	0%
<i>hsp150</i>	1/100	1%
<i>rvs161</i>	0/100	0%
<i>sam37</i>	3/100	3%
<i>vma7</i>	1/100	1%
<i>vph2/ykl118w</i>	0/100	0%
<u>Mitochondrial Proteins</u>		
<i>atp2</i>	6/100	6%
<i>img2</i>	0/100	0%
<i>mct1</i>	12/100	12%
<i>ygl218w/mdm34</i>	3/100	3%
<i>mrps35</i>	0/100	0%
<i>rsm7/yjr114w</i>	4/72	5.6%
<i>sco1</i>	2/100	3%
<u>Other</u>		
<i>ydr417c/rpl12b</i>	4/100	4%
<i>srv2</i>	0/100	0%
<i>ado1</i>	0/33	0%
<i>lip5</i>	33/100	33%
<i>ids2</i>	1/100	1%
<i>bud19/rpl39</i>	0/100	0%
<i>ybr099c-1</i>	1/100	1%
<i>och1</i>	1/100	1%
<i>psy1/ykl075c</i>	0/100	0%
<i>rpl31a</i>	0/100	0%
<i>ynr068c</i>	1/100	1%
<i>adk1</i>	5/73	6.8%
<i>gnd1/yhr182c-a</i>	5/100	5%
<i>slm4</i>	0/100	0%

DSB repair accuracy was tested a second time for mutants that exhibited > 5%

Ura⁻ cells. This was done to ensure reproducibility. For the second round of testing, each

mutant was separately transformed with NcoI-cut pRS315URA3 4 times and spread to glucose minus leucine plates. Fifty colonies from each transformation were then patched to glucose minus leucine (for control) and glucose minus uracil plates to detect Ura⁻ transformants. Averages were then calculated as shown in Table 13. Three mutant strains exhibited reproducible repair inaccuracy 3 times the wildtype level.

Table 13. Mutants with reduced DSB repair accuracy from first round of NHEJ testing were tested a second time.

Mutant	1st Test		2nd Test	
	Ura ⁻ /Leu ⁺	%	Ura ⁻ /Leu ⁺ ^a	%
WT	0/100	0%	0.25	0.5%
<i>adk1</i>	5/73	6.8%	0.25	0.5%
<i>atp2</i>	6/100	6%	0.5	1.0%
<i>gnd4/yhr182c-a</i>	5/100	5%	0.5	1.0%
<i>lip5</i>	33/100	33%	0	0%
<i>lsm7</i>	14/100	14%	1	2.0%
<i>mct1</i>	12/100	12%	2	4.0%
<i>mms22</i>	15/100	15%	0.25	0.5%
<i>rsm7/yjr114w</i>	4/72	5.6%	0	0%
<i>rtf1</i>	7/100	7%	0.75	1.5%
<i>rtt109 (rem50)</i>	3/40	7.5%	0.5	1.0%
<i>spt20</i>	11/100	11%	0	0%

^a Average Ura⁻/50 Leu⁺

Lsm7 is a “like”-SM protein involved in RNA processing (83). SM proteins comprise a stable SM core of small nuclear ribonucleic proteins that participate in mRNA splicing. Lsm proteins also aid in mRNA splicing as well as de-capping (84, 85). mRNA de-capping induces rapid degradation of the RNA molecule by exposing a 5’ monophosphate for hydrolysis. Because Lsm proteins contain nuclease functionality, Lsm7 might indirectly affect NHEJ accuracy by its effect on proper mRNA processing of genes more directly involved in repair.

Rtf1 is a protein involved in transcription by aiding in regulation of the TATA-box-binding protein (TBP) (86). TBP binding promotes RNA Polymerase II activity by recruitment from the Paf1 complex (87, 88). In addition to transcriptional regulation, Rtf1 is also necessary for indirect histone modification. Chromatin remodeling protein (Chd1) is recruited by Rtf1 propagating covalent modifications to histone proteins (89). Because Rtf1 is important for transcriptional regulation and histone modification, NHEJ protein expression may be indirectly regulated by either of those processes.

Based on our screening, Mct1 is necessary for both efficient and accurate repair via the NHEJ pathway. It is peculiar that a gene that codes for a mitochondrial protein exhibit reduced NHEJ accuracy. Further studies are needed to understand why compromised mitochondria provide a reduced ability to repair DSBs through the NHEJ pathway.

Another measure to further confirm the NHEJ repair defect of *EcoRI*^S mutants is to create knock-out strains in the lab. This is done through PCR-mediated gene disruption. We used this tool in conjunction with testing library mutant strains to confirm what is seen in initial screening processes. *arp5* is a strain that showed a reproducible decrease in NHEJ efficiency. Opposite mating type testing also corroborated our results. The next step in our analysis was to test a new knock-out strain of *arp5*. *arp5* inactivation was attempted by inserting the antibiotic resistance marker G418^r using pFA6MX4 into the *Arp5* gene in WT cells. The G418^r marker was amplified with flanking *ARP5* primers using PCR. To ensure that the G418^r would excise the *ARP5* gene, primers were designed with ~50 nt of sequence homology to *ARP5* and 25 nt that annealed specifically to the

pFA6MX4 plasmid. An example of the products generated by this PCR is shown in Figure 13.

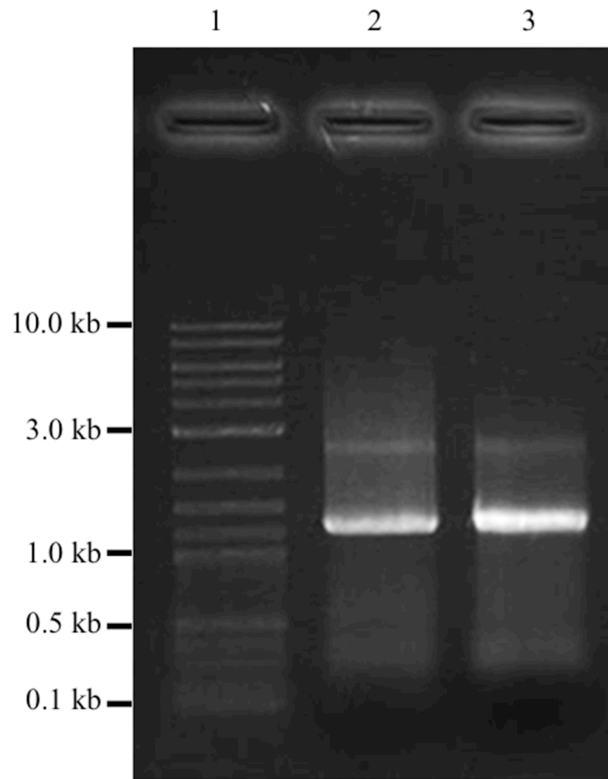


Figure 13. Agarose gel electrophoresis after PCR amplification of pFA6MX4 containing G418^r with 5' and 3' *ARP5* primers. Lane 1. 2-Log DNA ladder. Lanes 2-3. PCR product of pFA6MX4 containing G418^r amplified with gArp5a and gArp5b primers.

The G418^r gene was inserted into the *ARP5* region through homologous recombination. Because the G418^r gene was flanked with *ARP5* primers, there exists sequence homology between the surrounding regions of the G418^r gene and the *ARP5* gene itself in the chromosome. This permits homologous recombination (HR) to take place between the chromosomal *ARP5* gene and the G418^r fragment, effectively knocking out the *ARP5* gene. After HR completion, cells become *arp5*Δ::G418^r (Figure 14).

Transformed cells were spread onto non-selective YPDA plates to initiate generalized growth of all cells. Replica plating using YPDA + G418 antibiotic created a mirror image of the initial plate but with selection only for G418^r cells. The resulting colonies were then streak purified and subjected to chromosomal DNA purification.

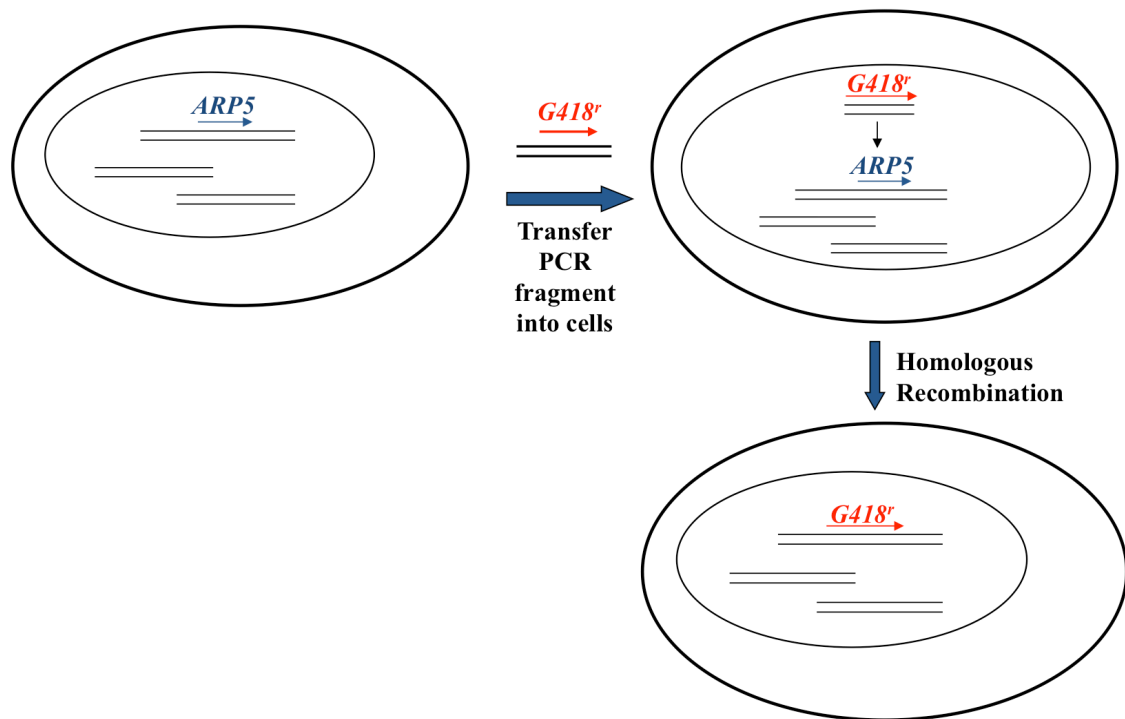


Figure 14. Inactivation of a gene (*ARP5*) by insertion of an antibiotic resistant marker (*G418^r*). WT cells were transformed with G418^r PCR fragments. G418^r was incorporated into *Arp5* via HR. Resulting cells are *arp5Δ::G418^r*.

Chromosomal DNA underwent a second PCR amplification to confirm gene knockout using test primers that anneal to the outside of the *ARP5* ORF (5' and 3' test primers). PCR fragments were compared to WT using agarose gel electrophoresis. The WT PCR product had a size of 2592 bp and the gene with G418^r gene inserted should be

1977 bp. The first attempt at *ARP5* knockout. All PCR fragments (Lanes 3-11) were the same size as WT (Lane 2) (Figure 15).

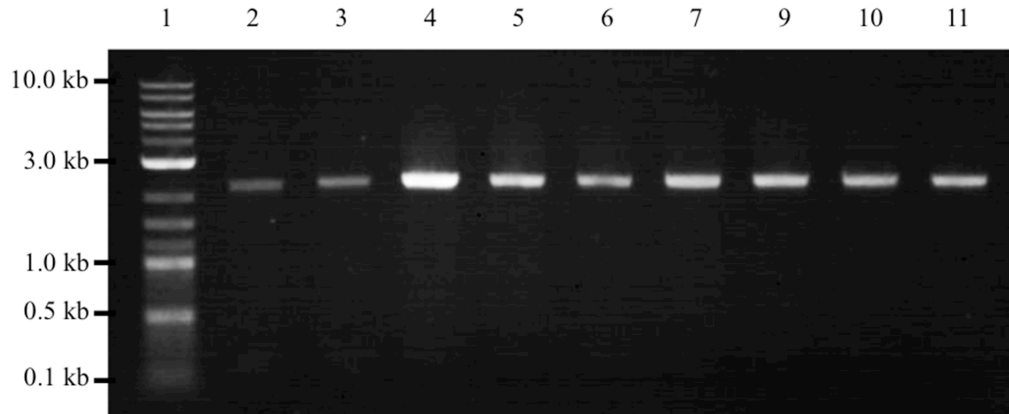


Figure 15. Agarose gel electrophoresis of PCR fragments from G418^r genomic DNA. Lane 1, 2-log ladder; Lane 2, WT PCR fragment using *arp5* test primers; Lanes 3-11, PCR fragments from G418^r genomic DNA amplification using *arp5* test primers. Fragments were run on a 0.9% gel.

The experiment was repeated again using previous PCR amplification products of the pFA6MX4 plasmid containing the G418^r marker. The PCR products were transformed into WT cells again. Chromosomal DNA preparations from six separate G418^r colonies were subjected to PCR using *arp5* test primers. Agarose gel electrophoresis illustrated the same results as seen above. It is unclear as to the cause of this failure, but it is possible that the gA_{arp5} primers contain sequence homology with another section of a yeast chromosome and are being preferentially targeted to that location.

Another aspect of this study was to further characterize the most interesting of the new EcoRI^S mutant strains. Our experiments with the vast majority of the 73 mutant strains did not suggest a role in NHEJ repair. Similarly, only 16 mutant strains exhibited a significant change (2x or greater) in DNA repair via the homologous recombination pathway, though only 48 of the 73 mutants were screened by graduate student Brian Sanderson. *mms22* mutants displayed sensitivity to EcoRI, MMS, bleomycin, and gamma radiation in the initial screen in our lab (13). They also exhibited 2.2 fold decrease in plasmid:recombination (80) and an average of 2.3 fold decrease in NHEJ repair. *MMS22* is a gene that codes for a protein involved in chromosome stability/segregation. Specifically, Mms22 is a subunit of the E3 ubiquitin ligase complex involved in DNA replication and repair. With Mms1, Mms22 helps to stabilize the replisome that is often susceptible to DNA damage (90).

To further characterize the role of this complex in DSB repair, we looked at several proteins involved in Mms22-dependent DNA repair. Of these, Mms1, Rtt107, and Rtt101 were analyzed. Mms1 is another subunit of the E3 ubiquitin complex, that localizes at stalled replication forks (90). In a high-throughput mass spectroscopy study, Rtt101 and Rtt107 proteins were found to bind with Mms22 (56) and they also exhibit an epistatic relationship to Mms22 (91).

mm22, *mms1*, *rtt101*, and *rtt107* cells were transformed with pGalEcoRI or pRS316 plasmids and spread onto glucose minus uracil (Glu-Ura) plates. The *GAL1* promoter on the pGalEcoRI plasmid is strongly transcriptionally repressed by glucose. Colonies of each plasmid assay from Glu-Ura plates were then patched onto 2% raffinose minus uracil (Raff-Ura) plates. Raffinose delivers no glucose repression but there is also

no *GAL4* activator protein, so the *GAL* promoter has very low activity. This step is necessary (instead of going from Glu-Ura to galactose-uracil (Gal-Ura) to encourage fast induction, otherwise, cells would have to overcome glucose repression). pGalEcoRI and pRS316 transformed cells were then pronged onto Gal-Ura plates in a serial dilution array (Figure 16). On Gal-Ura plates, the glucose repressor proteins are not on the DNA and Gal4 activator proteins strongly induce RNA polymerase binding to the promoter. This promotion leads to EcoRI expression in the cell, creating DSBs.

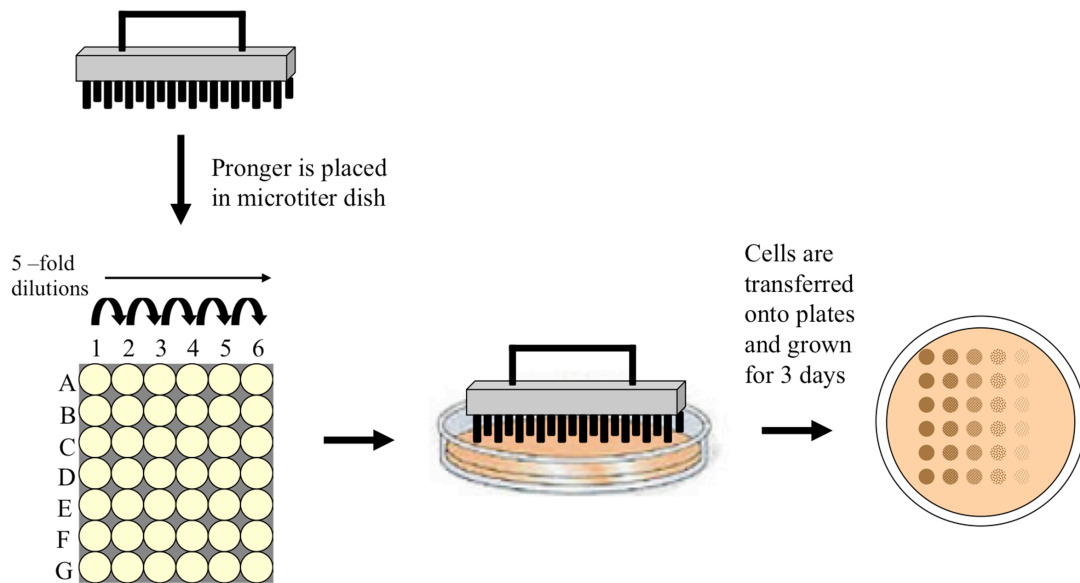


Figure 16. Dilution pronging assay to quantitate *Mms22*-complex DNA repair mutants. *mms22*, *mms1*, *rtt101*, and *rtt107* were pronged onto Raff-Ura and Gal-Ura plates to measure repair capabilities in cells with *in vivo* expression of EcoRI by the *GAL* promoter system. Each assay was performed with WT (BY4742) and *rad50* cells. pRS316 transformants acted as a baseline standard for transformation efficiency of each assay.

Pronging studies were performed from cells harvested from Raff-Ura patches. For each assay, BY4742 and *rad50* cells were included and for each strain cells with incorporated pRS316 vector or pGalEcoRI are compared. Initial survival studies were

tested using only 2% Raff-Ura and 2% Gal-Ura plates, but EcoRI induction was too strong, producing an unexpectedly high level of growth inhibition in WT cells. To reconcile this problem, strains were also pronged onto 1% Raff + 2% Gal-Ura and 0.1% Raff + 2% Gal-Ura to promote slower induction of EcoRI expression and provide a better illustration of killing effects. *mms22* cells were killed in all plates containing galactose (Figure 17). Although the growth rates (colony diameters) of *mms1* mutants were reduced when EcoRI was expressed, no killing was observed in *mms1*, *rtt101*, or *rtt107* mutants.

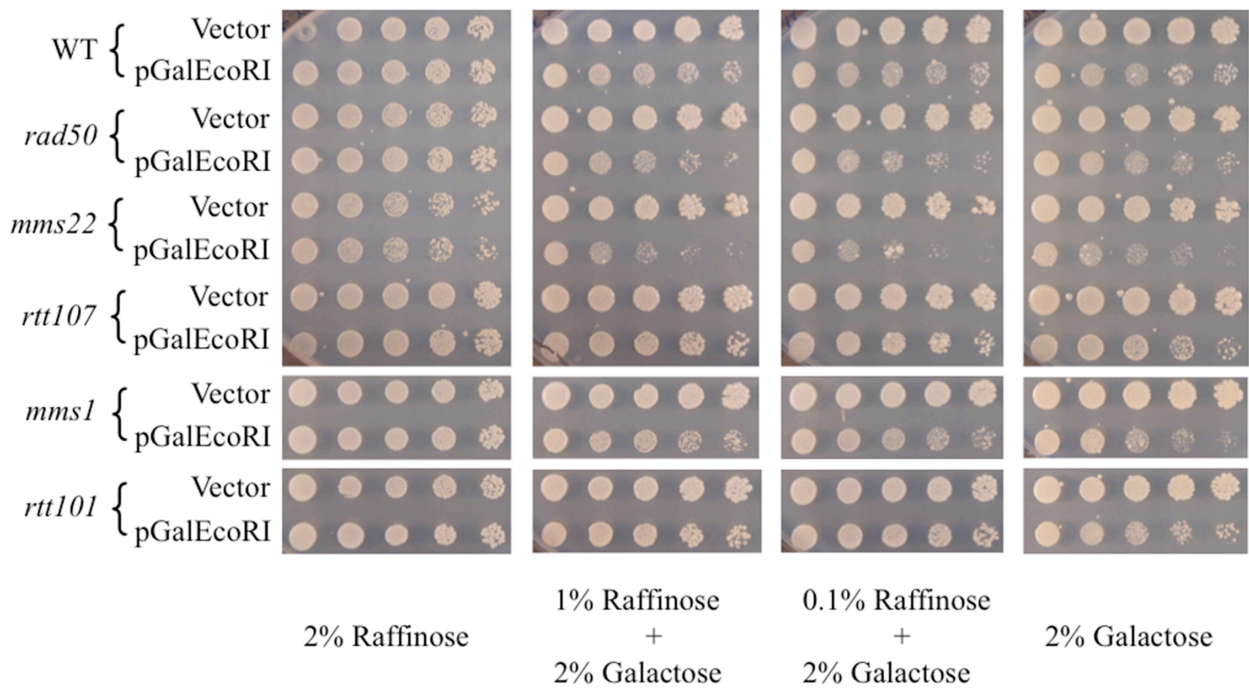


Figure 17. Survival of library *mms22*, *rtt107*, *mms1*, *rtt101* mutants after induction of EcoRI expression. Cells were serially diluted 5-fold and pronged onto plates.

The McKinney *et al.* study showed that *mms22* mutants were sensitive to EcoRI, MMS, and bleomycin (13). The next aspect of elucidating Mms22 group proteins' roles was to determine sensitivity to MMS and bleomycin. Using *rad50* as a negative control, *mms22*, *mms1*, *rtt101*, and *rtt107* cells were all subjected to serial dilution killing studies

with 1 mM MMS, 2 mM MMS, 2 $\mu\text{g}/\text{mL}$ bleomycin, and 4 $\mu\text{g}/\text{mL}$ bleomycin in YPDA media (Figure 18). *mms22* cells exhibited reduced survival with 1 mM and 2 mM MMS but *mms1*, *rtt101*, and *rtt107* cells were relatively unaffected. Only 2 $\mu\text{g}/\text{mL}$ bleomycin is shown in Figure 17 because there was no growth from any strain on 4 $\mu\text{g}/\text{mL}$ bleomycin plates. *rad50* cells were very sensitive to 2 $\mu\text{g}/\text{mL}$ bleomycin, thus, the absence of its growth. Relative to WT, *mms22* mutants showed a large reduction in growth rates with 2 $\mu\text{g}/\text{mL}$ bleomycin. *mms1* and *rtt101* cells exhibited a modestly reduced number of colonies in the 3rd dilution (3rd column in the right panel of Figure 18), indicating that they are only moderately sensitive to bleomycin. The results in Figure 14 and 15 indicate that the other subunits of the Mms22 protein complex, Mms1, Rtt101, and Rtt107 do not play important roles in repair of DSBs. Thus, even though previous studies have suggested that these three proteins work with Mms22 as part of the E3 ubiquitin ligase complex to influence DNA replication and repair (55-58), our results suggest that they are largely dispensable for functions of Mms22.

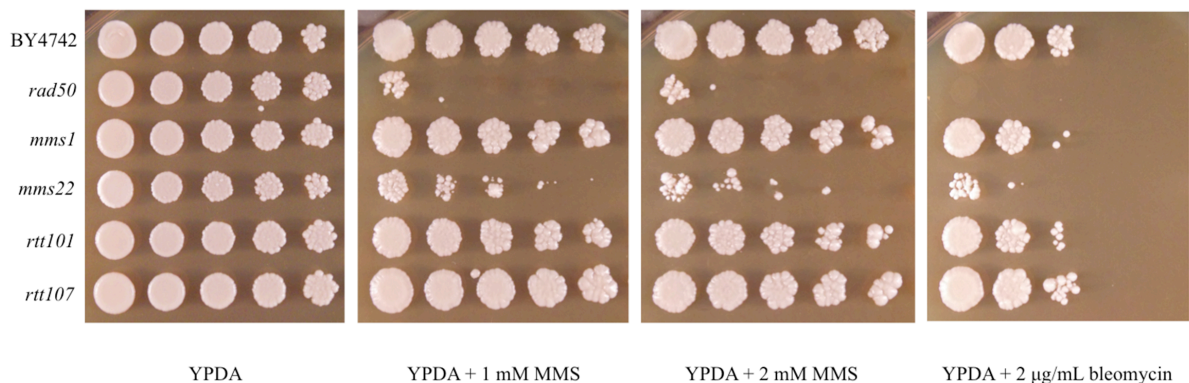


Figure 18. Survival of library *mms22*, *rtt107*, *mms1*, and, *rtt101* mutants on MMS and bleomycin. Cells were serially diluted 5-fold and pronged onto plates.

CHAPTER IV

Summary and Conclusions

The purpose of this project was to analyze 73 EcoRI^s mutants for DSB repair efficiency and accuracy through the NHEJ pathway. The 73 EcoRI^s strains are part of a larger screening of 211 diploid library strains that were sensitive to gamma radiation. Gamma radiation is known to damage DNA and can have disastrous effects on the cell if the lesions are not repaired. Further investigation into the gamma^s strains showed that 81 of them were also sensitive to EcoRI expression. EcoRI causes DSBs, exclusively, implying that strains sensitive to EcoRI expression play a role in DSB repair.

Recently, our lab has developed a modified early stationary phase yeast cell transformation protocol that has increased transformation efficiency. Using this new protocol, larger differences between known NHEJ mutants in repair efficiencies were seen than in past studies. This finding illustrates a difference in the degree of importance each protein complex plays in the NHEJ repair pathway that has not been seen before.

An important part of this project was to sift through the literature and determine the levels of fold reduction in known NHEJ mutants (*yku70*, *yku80*, *dnl4*, *lif1*, *nej1*, *mre11*, *rad50*) in past studies to create a reference for known repair efficiencies. The median reduction in plasmid NHEJ repair ranged from 11.5-20 fold in the past studies. These results imply that there is no strong difference between *yku* mutants, *mrx* mutants, and DNA ligase IV mutants i.e., each of the 3 major NHEJ complexes are apparently equally important for repair of a DSB. Values found in our lab indicated a > 600 fold

reduction in *yku* mutants, a 6-8 fold reduction in *mrx* mutants, and a 700-1000 fold decrease in DNA ligase IV mutants. These results demonstrate that the new transformation protocol used in conjunction with plasmid pRS315URA3 was able to make critical distinctions between the roles of each complex that were not detectable before.

Using our new improved assay, we tested the 73 EcoRI^s strains implicated in DSB repair. Extensive screening and opposite mating type testing found three mutant strains to exhibit ≥ 3 fold reduction in DSB repair efficiency relative to WT cells. Two mutants contained defective genes that coded for nuclear functioning proteins. *BUD32* is a gene that codes for a protein kinase that has been linked to telomere capping and length regulation. *bud32* cells had a 4 fold decrease relative to WT cells. *ARP5* encodes an actin-related protein that interacts with histone proteins and has been linked to transcription; *arp5* cells exhibited a reduction in repair efficiency of 7 fold. *mct1* is the last mutant strain with reduced repair efficiency. The product of this gene is involved in mitochondrial fatty acid synthesis. *mct1* cells had a 13 fold decrease in NHEJ repair efficiency, but further studies are needed to determine how a mitochondrial protein might affect DSB repair.

In addition to NHEJ repair efficiency, accuracy was also tested in the 73 EcoRI^s mutant strains. Testing found that three mutants had ≥ 3 fold reduction in repair accuracy relative to WT cells. Interestingly, *mct1* was the only strain deficient in both repair efficiency and accuracy. Two mutants coding for a nuclear protein were found to have reduced NHEJ repair accuracy, *rtf1* and *lsm7*. *Rtf1* is involved in transcriptional regulation by influencing the TATA-box-binding protein that helps promote RNA

Polymerase II. Lsm7 is a protein with nuclease functionality that is known to be involved in mRNA processing. A possible role for this protein in DNA processes has not yet been tested.

The last aspect of this project was to investigate one of the most interesting mutants of the 73 EcoRI^s strains previously identified in the lab. Mms22 is in a complex with Mms1, Rtt101, and Rtt107 acting as an E3 ubiquitin ligase complex. *mms22* cells have already been shown to be sensitive to MMS, bleomycin, and EcoRI. *rtt101*, *rtt107*, and *mms1* mutants were subjected to survival studies of *in vivo* EcoRI expression and it was found that they were not EcoRI^s. Additionally, these mutants were subjected to MMS and bleomycin survival tests. They did not show sensitivity to MMS and were only moderately affected by bleomycin. These results indicate that, although Rtt101, Rtt107, and Mms1 corroborate with Mms22 for protein ubiquitination, they play no major role in DSB repair with Mms22.

REFERENCES

1. Frankenberg, D.; Frankenberg-Schwager, M.; Blöcher, D.; Harbich, R. *Radiation Res.* **1981**, *88*, 524-532.
2. Obe, G.; Johannes, C.; Schulte-Frohlinde, D. *Mutagenesis.* **1992**, *7*, 3-12.
3. Sreedhara, A.; Cowan, J.A., *J. Biol. Inorg. Chem.* **2001**, *6*, 337-347.
4. Xiao, W.; Chow, B. L.; Rathgeber, L. *Curr. Genet.* **1996**, *30*, 461-468.
5. Takata, M.; Sasaki, M.S.; Sonoda, E.; Morrison, C.; Hashimoto, M.; Utsumi, H.; Yamaguchi-Iwai, Y.; Shinohara, A.; Takeda, S. *EMBO J.* **1998**, *17*, 5497-5508.
6. Frankenberg-Schwager, M.; Frankenberg, D. *Int. J. Radiat. Biol.* **1990**, *58*, 569-575.
7. Hefferin, M. L.; Tomkinson, A. E. *DNA Repair (Amst)* **2005**, *4*, 639-648.
8. Daley, J. M.; Palmbo, P.; Wu, D.; Wilson, T. E. *Annu. Rev. Genet.* **2005**, *39* 431-451.
9. Goffeau, A.; Barrell, B. G.; Bussey, H.; Davis, R. W.; Dujon, B.; Feldmann, H.; Galibert, F.; Hoheisel, J. D.; Jacq, C.; Johnston, M.; Louis, E. J.; Mewes, H. W.; Murakami, Y.; Philippsen, P.; Tettelin, H.; Oliver, S. G. *Science* **1996**, *274*, 563-567.
10. Boulton, S. J.; Jackson, S. P. *EMBO J.* **1996**, *15*, 5093-5103.
11. Chen, L.; Trujillo, K.; Ramos, W.; Sung, P.; Tomkinson, A. E. *Mol. Cell* **2001**, *8*, 1105-1115.
12. Paull, T.; Gellert M. *Proc. Natl. Acad. Sci. U.S.A.* **2000**, *97*, 6409-6414.
13. McKinney, J. S.; Sethi, S.; Tripp, J. D.; Nguyen, T. N.; Sanderson, B. A.; Westmoreland, J. W.; Resnick, M. A.; Lewis, L. K. *BMC Genomics* **2003**, *14*, 251-265.
14. Hefferin, M. L.; Tomkinson, A. E. *DNA Repair (Amst).* **2005**, *4*, 639-648.
15. Mimitou, E. P.; Symington, L.S. *Trends Biochem. Sci.* **2009**, *34*, 264-272.
16. San Filippo, J.; Sung, P.; Klein, H. *Annu. Rev. Biochem.* **2008**, *77*, 229-257.

17. Bennett, C.B.; Lewis, L. K.; Karthikeyan, G.; Lobachev, K. S.; Jin, Y. H.; Sterling, J. F.; Snipe J. R.; Resnick, M. A. *Genetics* **2001**, *29*, 426-434.
18. Game, J. C.; Birrell, G. W.; Brown, J. A.; Shibata, T.; Baccari, C.; Chu, A. M.; Williamson, M. S.; Brown, J. M. *Radiat Res* **2001**, *160*, 14-24.
19. Lewis, L. K.; Karthikeyan, G.; Cassiano, J.; Resnick, M. A. *Nucleic Acids Res.* **2005**, *33*, 4928-4939.
20. Tripp, J. D.; Lilley J. L.; Wood W. N.; Lewis L.K. *Yeast* **2013**, *30*, 191–200.
21. Boulton, S. B.; Jackson, S. P. *Nucleic Acids Res.* **1996**, *24*, 4639-4648.
22. Boulton, S. J.; Jackson, S. P. *EMBO J.* **1996**, *15*, 5093-5103.
23. Milne, G. T.; Jin, S.; Shannon, K. B.; Weaver, D. T. *Mol. and Cell. Biol.* **1996**, *16*, 4189-4198.
24. Tsukamoto, Y.; Kato, J.; Ikeda, H. *Letters to Nature*, **1997**, *388*, 900-903.
25. Schar, P.; Herrmann, G.; Daly, G.; Lindahl, T. *Genes & Devel.* **1997**, *11*, 1912-1924.
26. Lee S. E.; Paques, F.; Sylvan, J.; Haber, J. E. *Curr. Biol.* **1999**, *9*, 767-770.
27. Ooi, S. L.; Shoemaker, D. D.; Boeke, J. D. *Science* **2001**, *294*, 2552-2556.
28. Lewis, L. K.; Karthikeyan, G.; Westmoreland, J. W.; Resnick, M. A. *Genetics* **2001**, *160*, 49-62.
29. Valencia, M.; Bentele, M.; Vaze, M. B.; Herrmann, G.; Kraus, E.; Lee, S. E.; Schar, P.; Haber, J. E. *Letters to Nature* **2001**, *414*, 666-669.
30. Kegel, A.; Sjöstrand, J. O. O.; Åström, S. U. *Curr. Biol.* **2001**, *11*, 1611-1617.
31. Erdemir, T.; Bilican, B.; Cagatay, T.; Goding, C. R.; Yavuzer, U. *Mol. Microbiol.* **2002**, *46*, 947-957.
32. Karathanasis, E.; Wilson, T. E. *Genetics* **2002**, *161*, 1015-1027.
33. Lewis, L. K.; Storici, F.; Van Komen, S.; Calero, S.; Sung, P.; Resnick, M. A. *Genetics.* **2004**, *166*, 1701-1713.
34. Jazayeri, A; McAinsh, A. D.; Jackson, S. P. *PNAS* **2004**, *101*, 1644-1649.
35. Schar, P.; Fasi, M.; Jessberger, R. *Nucleic Acids Res.* **2004**, *32*, 3921-3929.

36. Daley, J. M.; Wilson, T. E. *Molec. and Cell Biol.* **2004**, *25*, 896-906.
37. Virgilio, M. D.; Gautier, J. *J. Cell Biol.* **2005**, *171*, 765-771.
38. Zhang, X.; Paull, T. T. *DNA Repair* **2005**, *4*, 1281-1294.
39. Lewis, L. K.; Karthikeyan, G.; Cassiano, J.; Resnick, M. A. *Nucleic Acids Res.* **2005**, *33*, 4928-4939.
40. Shim, E. Y.; Ma, J.; Oum, J.; Yanez, Y.; Lee, S. E. *Molec. and Cell Biol.* **2005**, *25*, 3934-3944.
41. Bilsland, E.; Hult, M.; Bell, S. D.; Sunnerhagen, P.; Downs, J. A. **2007**, *6*, 1471-1484.
42. Herrmann, G.; Kais, S.; Hoffbauer, J.; Shah-Hosseini, K.; Bruggenolte, N.; Schober, H.; Fasi, M.; Schar, P. *Nucleic Acids Res.* **2007**, *35*, 2321-2332.
43. Jessulat, M.; Alamgir, M.; Salsali, H.; Greenblatt, J.; Xu, J.; Golshani, A. *A. Biochem. and Biophys.* **2008**, *469*, 157-164.
44. Pitre, S.; North, C.; Alamgir, M.; Jessulat, M.; Chan, A.; Luo, X.; Green, J. R.; Dumontier, M.; Dehne, F.; Golshani, A. *Nucleic Acids Res.* **2008**, *36*, 4286-4294.
45. Palmbo, P. L.; Wu, D.; Daley, J. M.; Wilson, T. E. *Genetics* **2008**, *180*, 1809-1819.
46. Carter, S. D.; Viganova, D.; Chen, J.; Chovanec, M.; Astrom, S. U. *PNAS* **2009**, *106*, 12037-12042.
47. Bahmed, K.; Nitiss, K. C.; Nitiss, J. L. *PNAS* **2010**, *107*, 4057-4062.
48. Chen, X.; Tomkinson, A. E. *J. Biol. Chem.* **2010**, *286*, 4931-4940.
49. Tao, R.; Chen, H.; Gao, C.; Xue, P.; Yang, F.; Han, J. J.; Zhou, B.; Chen, Y. *Cell Res.* **2011**, *21*, 1619-1633.
50. Hohl, M.; Kwon, Y.; Galvan, S. M.; Xue, X.; Tous, C.; Aguilera, A.; Sung, P.; Petrini, J. H. *J. Nature Struc. Molec. Biol.* **2011**, *18*, 1124-1132.
51. Bahmed, K.; Seth, A.; Nitiss, K. C.; Nitiss, J. L. *Nucleic Acids Res.* **2011**, *39*, 970-978.
52. Srividya, I.; Tirupataiah, S.; Mishra, K. *PlosOne* **2012**, *7*, e31288.

53. Matsuzaki, K.; Terasawa, M.; Iwasaki, D.; Higashide, M.; Shinohara, M. *Genes-to-Cells* **2012**, *17*, 473-493.
54. Daley, J. M.; Palmbo, P.L.; Wu D.; Wilson, T.E. *Annu. Reve. Genet.* **2005**, *39*, 431-451.
55. Vaisica, J. A.; Baryshnikova A.; Costanzo, M.; Boone, C.; Brown G. W. *Mol. Biol. Cell* **2011**, *22*, 2396-2408.
56. Ho, Y.; Gruhler, A.; Heilbut, A.; Bader, G. D.; Moore, L.; Adams, S. L.; Millar, A.; Taylor, P.; Bennett, K.; Boutilier, K.; Yang, L.; Wolting, C.; Donaldson, I.; Schandorff, S.; Shewnarane, J.; Vo, M.; Taggart, J.; Goudreault, M.; Muskat, B.; Alfarano, C.; Dewar, D.; Lin, Z.; Michalickova, K.; Willems, A. R.; Sassi, H.; Nielsen, P. A.; Rasmussen, K. J.; Andersen, J. R.; Johansen, L. E.; Hansen, L. H.; Jespersen, H.; Podtelejnikov, A.; Nielsen, E.; Crawford, J.; Poulsen, V.; Sørensen, B. D.; Matthiesen, J.; Hendrickson, R. C.; Gleeson, F.; Pawson, T.; Moran, M. F.; Durocher, D.; Mann, M.; Hogue, C. W.; Figeys, D.; Tyers, M. *Nature* **2002**, *415*, 180-183.
57. Baldwin, E. L.; Berger, A. C.; Corbett, A. H.; Osheroff, N. *Nucleic Acids Res.* **2005**, *33*, 1021-1030.
58. Duro, E.; Vaisica, J. A.; Brown, G. W.; Rouse, J. *DNA Repair (Amst).* **2008**, *7*, 811-818.
59. Brachmann, C. B.; Davies, A.; Cost, G. J.; Caputo, E.; Li, J.; Hieter, P.; Boeke, J. D. *Yeast* **1998**, *14*, 115-132.
60. Sikorski, R. S.; Hieter, P. *Genetics* **1989**, *122*, 19-27.
61. Barnes, G.; Rine, J. *Proc. Natl. Acad. Sci. U.S.A.* **1985** *82*, 1354-1358.
62. Goldstein, A. L.; McCusker, J. H. *Yeast* **1999**, *15*, 1541-1553.
63. Soni, R.; Carmichael, J. P.; Murray J. A. *Curr. Genet.* **1993**, *24*, 455-459.
64. Chen, D. C.; Yang, B. C.; Kuo, T.T. *Curr. Genet.* **1992**, *21*, 83-84.
65. Werner - Washburne, M.; Braun, E. L.; Crawford, M. E.; Peck, V. M. *Mol. Microbiol.* **1996**, *19*, 1159-1166.
66. Gietz, R. D.; Schiestl, R. H.; Willems, A. R.; Woods, R. A. *Yeast* **1995**, *11*, 355-360.
67. Li, X.; Cai, M. *J. Biol. Chem.* **1999**, *274*, 24220-24231.

68. Verghese, J.; Abrams, J.; Wang, Y.; Morano, K. A. *Microbiol. Mol. Biol. Rev.* **2012**, *76*, 115-158.
69. Bennet, C. B.; Lewis, L. K.; Karthikeyan, G.; Lobachev, K. S.; Jin, Y. H.; Sterling, J. F.; Snipe, J. R.; Resnick, M. A. *Nat. Genet.* **2001**, *29*, 426-434.
70. Game J. C.; Birrell, G. W.; Brown, J. A.; Shibata, T.; Baccari, C.; Chu, A. M.; Williamson, M. S.; Brown, J. M. *Radiat. Res.* **2003**, *160*, 14-24.
71. Takeda, M.; Vassarotti, A.; Douglas, M. G. *J. Biol. Chem.* **1985**, *260*, 15458-15465.
72. Fedor-Chaikin, M.; Deschenes, R. J.; Broach, J. R. *Cell* **1990**, *61*, 329-340.
73. Perrochia, L.; Guetta, D.; Hecker, A.; Forterre, P.; Basta, T. *Nucleic Acids Res.* **2013**, *41*, 9484-9499.
74. Downey, M.; Houlsworth, R.; Maringele, L.; Rollie, A.; Brehme, M.; Galicia, S.; Guillard, S.; Partington, M.; Zubko, M. K.; Krogan, N. J.; Emili, A.; Greenblatt, J. F.; Harrington, L.; Lydall, D.; Durocher, D. *Cell* **2006**, *124*, 1155-1168.
75. Hu, Y.; Tang, H. B.; Liu, N. N.; Tong, X. J.; Dang, Y. M.; Fu, X. H.; Zhang, Y.; Peng, J.; Meng, F. L.; Zhou, J. Q. *PloS Genet.* **2013**, *9*, e1003208.
76. Shen, X.; Ranallo, R.; Choi, E.; Wu, C. *Molecular cell* **2003**, *12*, 147-155.
77. Yen, K.; Vinayachandran, V.; Batta, K.; Koerber, R. T.; Pugh, B. F. *Cell* **2012** *149*, 1461-1473
78. Schneider, R.; Brors, B.; Burger, F.; Camrath, S.; Weiss, H. *Curr Genet.* **1997**, *32*, 384-388.
79. Hiltunen, J. K.; Autio, K. J.; Schonauer, M. S.; Kursu, V. A.; Diekmann, C. L.; Kastaniotis, A. J. *Biochem. Biophys. Acta.* **2010**, *1797*, 1195-1202.
80. Sanderson, B. Investigation of the Functions of New Genes Involved in Repair of DNA Double-Strand Breaks in *Saccharomyces cerevisiae*. M. S. Thesis, Texas State University, San Marcos, TX 2013.
81. Lewis, L. K.; Resnick, M. A. *Mutation Research/Fundamental and Molecular Mechanisms of Mutagenesis*, **2000**, *451*, 71-89.
82. Betermier, M.; Bertrand, P.; Lopez, B. S. *PloS Genet.* **2014**, *1*, e1004086.
83. Beggs, J. D. (2005) *Biochem. Soc. Trans.* **2005**, *33*, 433-438.

84. He, W.; Parker, R. *Curr. Opin. Cell Biol.* **2000**, *12*, 346-50.
85. Tharun, S.; He, W.; Mayes, A. E.; Lennertz, P.; Beggs, J. D.; Parker, R. *Nature* **2000**, *404*, 515-518.
86. Stolinski, L.A.; Eisenmann, D. M.; Arndt, K. M. *Mol. Cell Biol.* **1997**, *17*, 4490-4500.
87. Mueller, C. L.; Jaehning, J. A. *Mol. Cell Biol.* **2002**, *22*, 1971-1980.
88. Warner, M. H.; Roinick, K. L., Arndt, K. M. *Mol. Cell Biol.* **2007**, *27*, 6103-6115.
89. Simic, R.; Lindstrom, D. L.; Tran, H. G.; Roinick, K. L.; Costa, P. J.; Johnson, A. D.; Hartzog, G. A.; Arndt, K. M. *EMBO* **2003**, *22*, 1846-1856.
90. Vaisica, J. A.; Baryshnikova, A.; Costanzo, M.; Boone, C.; Brown, G. W. *Mol. Biol. Cell* **2011**, *22*, 2396-2408.
91. Baldwin, E. L.; Berger, A. C.; Corbett, A. H.; Osheroff, N. *Nucleic Acids Res.* **2005**, *33*, 1021-1030.